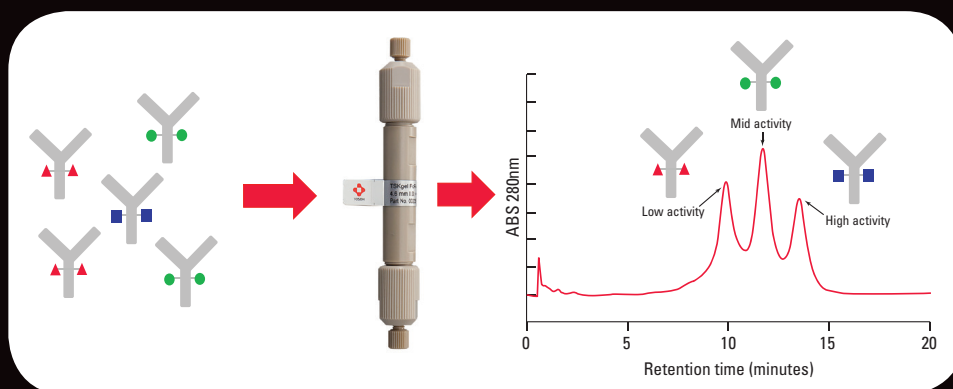


## TSKgel® FcR-IIIA-NPR Affinity Column

### A New Tool for Quick ADCC Activity Assessment

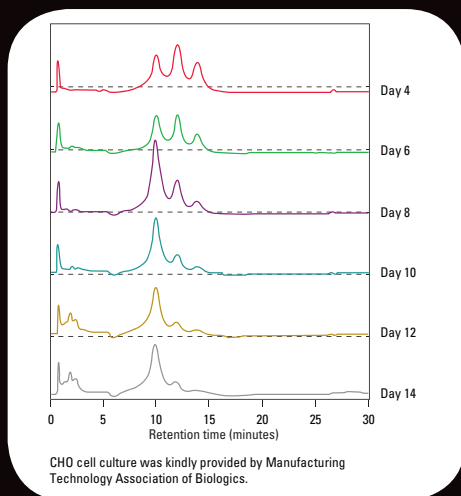


### Separation of mAb glycoforms according to their affinity to Fc receptor/ADCC activity

- Faster and less expensive than current ADCC activity assays
- Easy and reproducible HPLC analysis based on FcγIIIa receptor affinity of mAbs
- Unique glycoprotein elution profile of IgG allows assessment of ADCC activity

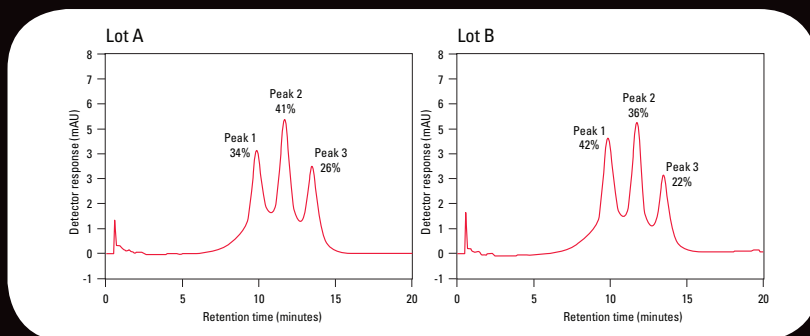
# TSKgel FcR-III A-NPR Affinity Column

## Cell culture monitoring



## Versatile Method Applicable to Both Purified Sample and Supernatant

## HPLC analysis of two lots of a therapeutic antibody



## Can be used in many phases of development and production:

- Cell line screening in early R&D
- Upstream development and optimization
- Lot-to-lot comparison in QC
- Biosimilar/originator comparison
- Monitoring of glycoengineering

TSKgel and Tosoh Bioscience are registered trademarks of Tosoh Corporation.

*Current Trends in*

# **MASS** **Spectrometry**

Volume 17 Number 5 May 2019  
[www.chromatographyonline.com](http://www.chromatographyonline.com)

**Analyzing Pesticides  
in Spinach Using  
GC×GC-TOF-MS**

**Flavonoid Profiling  
with a Structure-  
Based MS<sup>n</sup> Approach**

**Determination  
of Lurasidone  
Metabolites in Urine  
with Untargeted  
LC-HRMS**

Quadrupole Time-of-Flight  
Liquid Chromatograph Mass Spectrometer

# LCMS-9030



## Effortless Performance

Conduct Critical Qualitative and Quantitative Analysis with Genuine Confidence and Ease

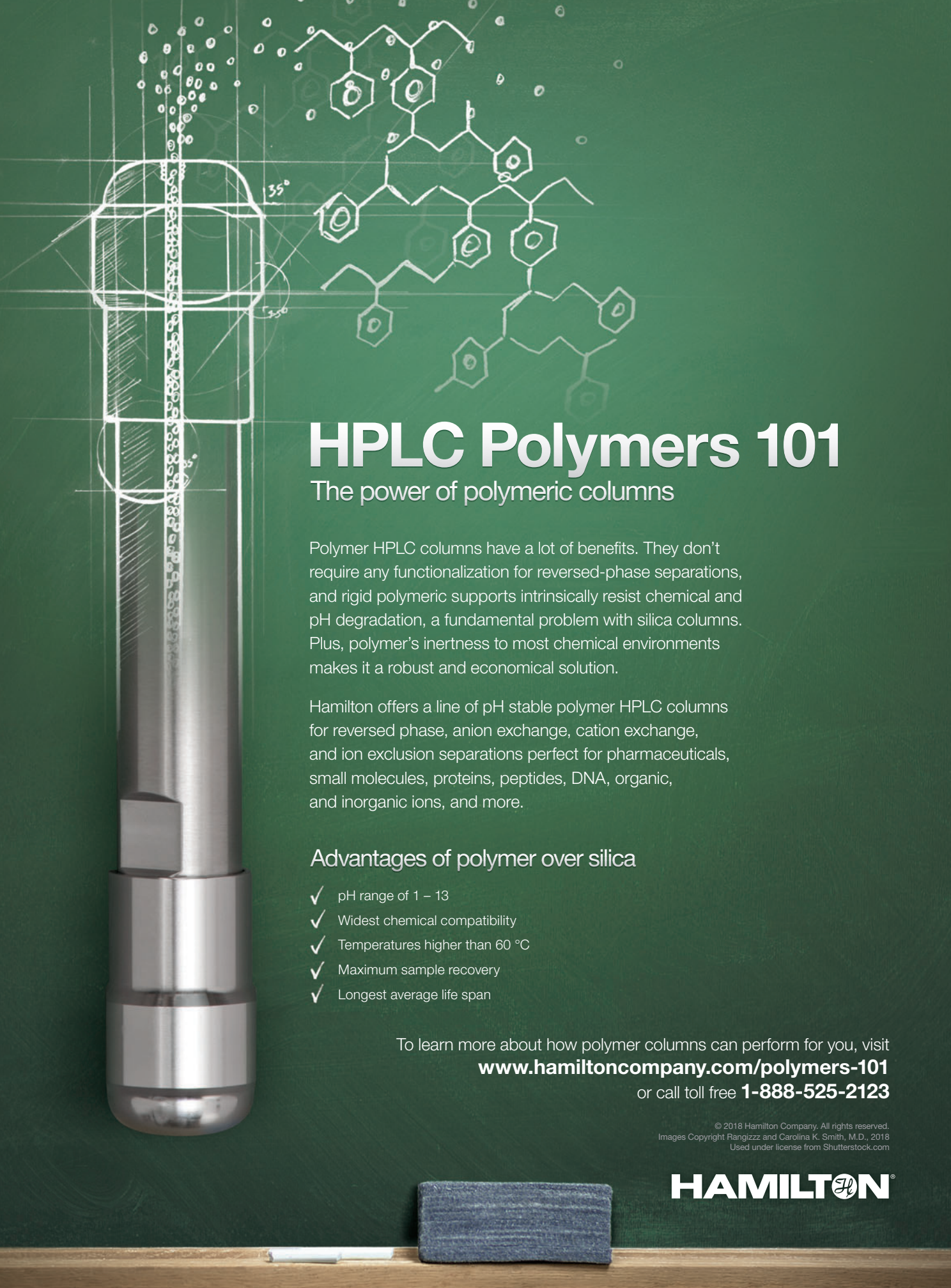
Shimadzu's research-grade **LCMS-9030 quadrupole time-of-flight (Q-TOF) mass spectrometer** combines the engineering DNA from our proven triple quadrupole (LC-MS/MS) platform with powerful, new TOF architecture to transform high mass accuracy workflows. The result is a system that delivers high-resolution, accurate-mass detection with incredibly fast data acquisition rates.



Learn more about Shimadzu's Q-TOF LCMS-9030.

Call (800) 477-1227 or visit us online at [www.ssi.shimadzu.com](http://www.ssi.shimadzu.com)

Shimadzu Scientific Instruments Inc., 7102 Riverwood Dr., Columbia, MD 21046, USA



# HPLC Polymers 101

## The power of polymeric columns

Polymer HPLC columns have a lot of benefits. They don't require any functionalization for reversed-phase separations, and rigid polymeric supports intrinsically resist chemical and pH degradation, a fundamental problem with silica columns. Plus, polymer's inertness to most chemical environments makes it a robust and economical solution.

Hamilton offers a line of pH stable polymer HPLC columns for reversed phase, anion exchange, cation exchange, and ion exclusion separations perfect for pharmaceuticals, small molecules, proteins, peptides, DNA, organic, and inorganic ions, and more.

### Advantages of polymer over silica

- ✓ pH range of 1 – 13
- ✓ Widest chemical compatibility
- ✓ Temperatures higher than 60 °C
- ✓ Maximum sample recovery
- ✓ Longest average life span

To learn more about how polymer columns can perform for you, visit

[www.hamiltoncompany.com/polymers-101](http://www.hamiltoncompany.com/polymers-101)

or call toll free **1-888-525-2123**

© 2018 Hamilton Company. All rights reserved.  
Images Copyright Pangizzz and Carolina K. Smith, M.D., 2018  
Used under license from Shutterstock.com

**HAMILTON**<sup>®</sup>



**MANUSCRIPTS:** To discuss possible article topics or obtain manuscript preparation guidelines, contact the editorial director at: (732) 346-3020, e-mail: LBush@mmhgroup.com. Publishers assume no responsibility for safety of artwork, photographs, or manuscripts. Every caution is taken to ensure accuracy, but publishers cannot accept responsibility for the information supplied herein or for any opinion expressed.

**CHANGE OF ADDRESS:** Send change of address to *LCCG North America*, P.O. Box 6196, Duluth, MN 55806-6196; provide old mailing label as well as new address; include ZIP or postal code. Allow 4–6 weeks for change.

**RETURN ALL UNDELIVERABLE CANADIAN ADDRESSES TO:** IMEX Global Solutions, P.O. Box 25542, London, ON N6C 6B2, CANADA. PUBLICATIONS MAIL AGREEMENT No.40612608.

**REPRINT SERVICES:** Reprints of all articles in this issue and past issues are available (500 minimum). Licensing and Reuse of Content: Contact our official partner, Wright's Media, about available usages, license fees, and award seal artwork at Advanstar@wrightsmedia.com for more information. Please note that Wright's Media is the only authorized company that we've partnered with for MultiMedia Healthcare materials.

**C.A.S.T. DATA AND LIST INFORMATION:** Contact Melissa Stillwell, (218) 740-6831; e-mail: MStillwell@mmhgroup.com

**INTERNATIONAL LICENSING:** Jillyn Frommer, (732) 346-3007, fax: (732) 647-1104; e-mail: JFrommer@mmhgroup.com



© 2019 MultiMedia Healthcare LLC All rights reserved. No part of this publication may be reproduced or transmitted in any form or by any means, electronic or mechanical including by photocopy, recording, or information storage and retrieval without permission in writing from the publisher. Authorization to photocopy items for internal/educational or personal use, or the internal/educational or personal use of specific clients is granted by MultiMedia Healthcare LLC for libraries and other users registered with the Copyright Clearance Center, 222 Rosewood Dr. Danvers, MA 01923, 978-750-8400 fax 978-646-8700 or visit <http://www.copyright.com> online. For uses beyond those listed above, please direct your written request to Permission Dept. fax 732-647-1104 or email: JFrommer@mmhgroup.com.

**MultiMedia Healthcare LLC** provides certain customer contact data (such as customers' names, addresses, phone numbers, and e-mail addresses) to third parties who wish to promote relevant products, services, and other opportunities that may be of interest to you. If you do not want MultiMedia Healthcare LLC to make your contact information available to third parties for marketing purposes, simply call toll-free 866-529-2922 between the hours of 7:30 a.m. and 5 p.m. CST and a customer service representative will assist you in removing your name from MultiMedia Healthcare LLC lists. Outside the U.S., please phone 218-740-6477.

**LCCG North America** does not verify any claims or other information appearing in any of the advertisements contained in the publication, and cannot take responsibility for any losses or other damages incurred by readers in reliance of such content.

**LCCG North America** welcomes unsolicited articles, manuscripts, photographs, illustrations and other materials but cannot be held responsible for their safekeeping or return.

485F US Highway One South, Suite 210  
Iselin, NJ 08830  
(732) 596-0276  
Fax: (732) 647-1235

**Michael J. Tessalone**  
Vice President/Group Publisher  
MTessalone@mmhgroup.com

**Stephanie Shaffer**

Publisher  
SShaffer@mmhgroup.com

**Edward Fantuzzi**

Associate Publisher  
EFantuzzi@mmhgroup.com

**Brianne Molnar**

Sales Manager  
BMolnar@mmhgroup.com

**Michael Kushner**

Senior Director, Digital Media  
MKushner@mmhgroup.com

**Laura Bush**

Editorial Director  
LBush@mmhgroup.com

**John Chasse**

Managing Editor  
JChasse@mmhgroup.com

**Jerome Workman**

Senior Technical Editor  
JWorkman@mmhgroup.com

**Cindy Delonas**

Associate Editor  
CDelonas@mmhgroup.com

**Kristen Moore**

Webcast Operations Manager  
KMoore@mmhgroup.com

**Vania Oliveira**

Project Manager  
VOliveira@mmhgroup.com

**Sabina Advani**

Digital Production Manager  
SAdvani@mmhgroup.com

**Kaylynn Chiarello-Ebner**

Managing Editor, Special Projects  
KEbner@mmhgroup.com

**Dan Ward**

Art Director  
dward@hcl.com

**Anne Lavigne**

Marketing Manager  
ALavigne@mmhgroup.com

**Melissa Stillwell**

C.A.S.T. Data and List Information  
MStillwell@mmhgroup.com

**Wright's Media**

Reprints  
Advanstar@wrightsmedia.com

**Jillyn Frommer**

Permissions  
JFrommer@mmhgroup.com

**Jesse Singer**

Production Manager  
jsinger@hcl.com

**Wendy Bong**

Audience Development Manager  
WBong@mmhgroup.com

**Matt Blake**

Audience Development Assistant Manager  
MBlake@mmhgroup.com

# A Higher Level of Sensitivity, Every Time.

High-purity UHPLC-MS LiChrosolv® solvents  
for rapid and reliable results.

**Because our high standards match yours:**

**[SigmaAldrich.com/UHPLC-MS](https://SigmaAldrich.com/UHPLC-MS)**



© 2019 Merck KGaA, Darmstadt, Germany and/or its affiliates.  
All Rights Reserved. MilliporeSigma, the vibrant M, Supelco and  
LiChrosolv are trademarks of Merck KGaA, Darmstadt, Germany  
or its affiliates. All other trademarks are the property of their  
respective owners. Detailed information on trademarks is available  
via publicly accessible resources.

2018 - 16505 02/2019

The life science business of  
Merck KGaA, Darmstadt,  
Germany operates as  
MilliporeSigma in the  
U.S. and Canada.

**Supelco®**  
Analytical Products

*Current Trends in***MASS****Spectrometry**

May 2019

## Articles

### **Determination of the Relative Prevalence of Lurasidone Metabolites in Urine Using Untargeted HRMS . . . . . 8**

**Erin C. Strickland, Jeffrey R. Enders, and Gregory L. McIntire**

For lurasidone treatment adherence testing, an untargeted high-resolution mass spectrometry method was employed, using known positive human urine samples to identify the lurasidone metabolites and their relative abundance in urine.

### **Quantitation and Nontargeted Identification of Pesticides in Spinach Extract with GC×GC–TOF–MS . . . . . 16**

**Todd Richards and Joseph Binkley**

In this study of pesticides in spinach extract, the use of GC×GC–TOF–MS is demonstrated as a methodology to overcome matrix interferences and quickly quantify suspected contaminants. The approach also allows nontargeted analysis using a single sample injection.

### **High-Throughput Structure-Based Profiling and Annotation of Flavonoids . . . . . 22**

**Simon Cubbon**

A novel mass spectrometry-based flavonoid profiling workflow is applied to characterize and structurally annotate a large number of unknown flavonoids in fruit juice and vegetable juice samples.

## Departments

### **Products . . . . . 29**

### **Ad Index . . . . . 30**

**Cover** image courtesy of tanchess - stock.adobe.com.

# Optimize your UHPLC instrumentation

Cheminert UHPLC injectors, switching valves, and selectors make it easy. Internal volume is minimized and dead volume is virtually eliminated. A proprietary rotor material and stator coating on some models achieve pressures to 20,000 psi, suitable for the most demanding analytical techniques. All models are compatible with any VICI actuation option.

- For high speed, high throughput, micro or nano flow UHPLC
- Pressures available in 10k, 15k, and 20k psi
- Bore sizes from 100-250  $\mu\text{m}$
- Fitting sizes available in 360  $\mu\text{m}$  to 1/16"
- Zero dead volume



**VICI**

[www.vici.com](http://www.vici.com)

For more information: [tech@vici.com](mailto:tech@vici.com)

# Determination of the Relative Prevalence of Lurasidone Metabolites in Urine Using Untargeted HRMS

Lurasidone is an atypical antipsychotic that was approved by the FDA in 2010 to treat bipolar depression and schizophrenia. Like other antipsychotics, adherence to lurasidone is critical for successful disease treatment. Thus, therapeutic drug monitoring (blood testing) is often employed by clinicians to monitor adherence. Urine drug testing, with its advantages over blood testing, is another method used to confirm medication adherence. However, analytes used in blood testing are often very different than those used for testing in urine, where nonactive metabolites are often most prevalent. Choosing metabolites in urine that are relatively prevalent affords optimal method sensitivity, and thus improved testing results for adherence. To ensure optimal lurasidone adherence testing, an untargeted high-resolution mass spectrometry method was employed, using known positive human urine samples to identify the lurasidone metabolites and their relative abundance in urine. This testing identified a different primary urine metabolite from what has been reported in blood. The higher prevalence of this metabolite will improve lurasidone urine adherence monitoring.

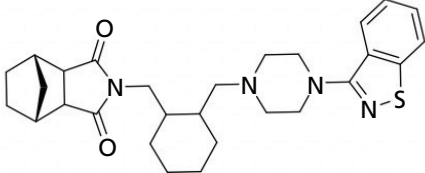
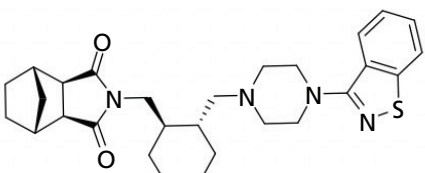
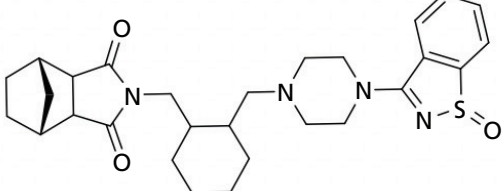
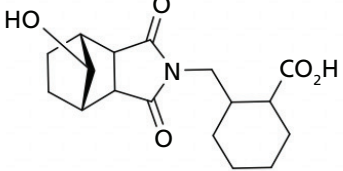
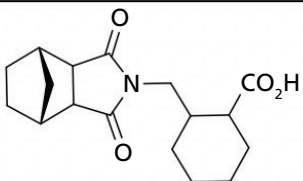
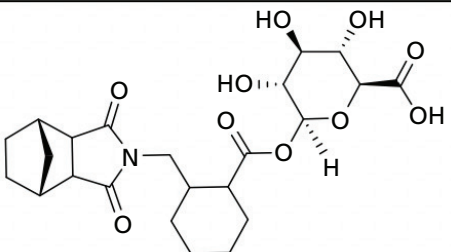
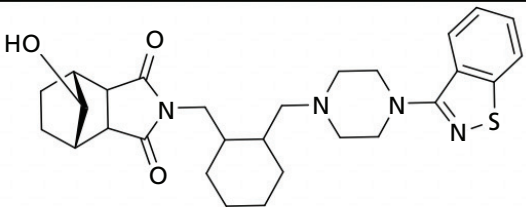
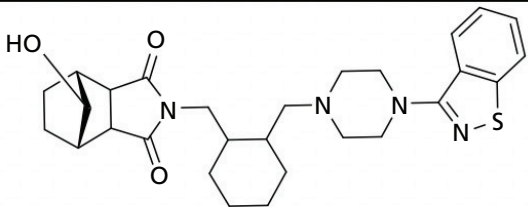
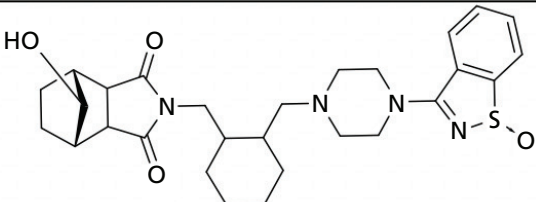
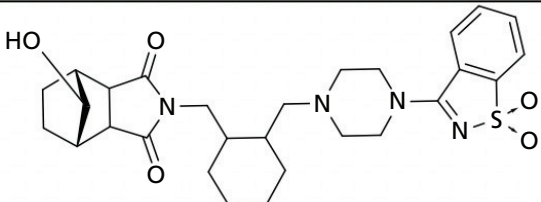
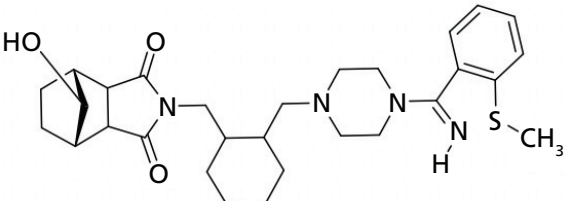
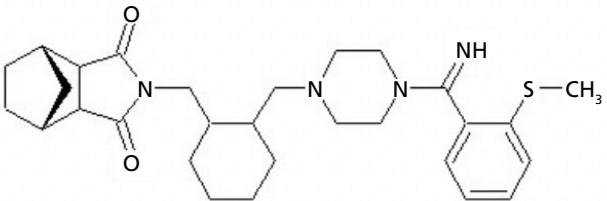
**Erin C. Strickland, Jeffrey R. Enders, and Gregory L. McIntire**

**M**edication monitoring has become increasingly important for successful treatment of patients with mental health diseases because adherence to treatment is generally poor, especially in the schizophrenic population (1–8). Urine has become an alternative to blood or plasma medication monitoring due to its noninvasive nature and ease of collection. Whereas blood or plasma drug testing usually involves the identification and quantitation of the parent compound or active metabolites, or both, the success of urine drug testing (UDT) is largely dependent on analysis of any metabolites of the parent compound. Although the parent compounds may be present in urine, often they are at very low concentrations relative to metabolites, and therefore do not provide the sensitivity required for medication monitoring. Urine metabolites are often predicted from identification in blood, plasma, or specific testing methods, such as gas chromatography–mass spectrometry (GC–MS), extractions, radioactivity, and using *in vitro* or animal samples. However, it has been shown that these methods are not always successful in identifying the most abundant urinary me-

tabolite (9–12). Without suitable metabolites to test, a negative UDT result could prompt a clinician to alter treatment for a patient when treatment need not be altered. Therefore, a generic, untargeted approach is useful for the successful identification of urinary metabolites suitable for highly sensitive medication monitoring. Liquid chromatography–high resolution mass spectrometry (LC–HRMS) provides a sensitive and nonspecific detection method for setting up such an experiment.

Lurasidone (Latuda) is an atypical antipsychotic that was approved for the treatment of acute symptoms of schizophrenia (13,14) and bipolar depression (15,16) in 2010 and 2013, respectively. It is commercially available as 20 mg, 40 mg, 60 mg, 80 mg, and 120 mg tablets, and is typically prescribed or administered at 40 or 80 mg per day. It is absorbed after oral administration with a bioavailability of 9–19%. Dosing is designed to be with food, which can increase the bioavailability by 100%. The mean elimination half-life is 18 h. Steady state serum concentrations for lurasidone are typically achieved after seven days of dosing (17–20).

**Table I: Structure of lurasidone and select metabolites**

 <p style="text-align: center;">(I)</p>	 <p style="text-align: center;">(II)</p>
Lurasidone (C <sub>28</sub> H <sub>36</sub> N <sub>4</sub> O <sub>2</sub> S), m/z = 493	
 <p>M10, ID-14324 (C<sub>28</sub>H<sub>36</sub>N<sub>4</sub>O<sub>3</sub>S), m/z = 509 <i>Lurasidone sulfoxide</i></p>	 <p>M5, ID 20220 (C<sub>17</sub>H<sub>23</sub>NO<sub>5</sub>), m/z = 322</p>
 <p>M11, ID-20219 (C<sub>17</sub>H<sub>23</sub>NO<sub>4</sub>), m/z = 306</p>	 <p>M7, M11 Glucuronide (C<sub>23</sub>H<sub>31</sub>NO<sub>10</sub>), m/z = 482</p>
 <p>M8, ID-14283 (exo-OH), (C<sub>28</sub>H<sub>35</sub>N<sub>4</sub>O<sub>3</sub>S), m/z = 509 <i>Hydroxylurasidone</i></p>	 <p>M9, ID-14326 (endo-OH), (C<sub>28</sub>H<sub>35</sub>N<sub>4</sub>O<sub>3</sub>S), m/z = 509 <i>Hydroxylurasidone</i></p>
 <p>ID-20221 (exo-OH) (C<sub>28</sub>H<sub>35</sub>N<sub>4</sub>O<sub>4</sub>S), m/z = 525</p>	 <p>ID-20222 (exo-OH) (C<sub>28</sub>H<sub>35</sub>N<sub>4</sub>O<sub>5</sub>S), m/z = 541</p>
 <p>M22 (C<sub>29</sub>H<sub>40</sub>N<sub>4</sub>O<sub>3</sub>S), m/z = 525 <i>S-Methyl hydroxylurasidone</i></p>	 <p>M21 (C<sub>29</sub>H<sub>40</sub>N<sub>4</sub>O<sub>2</sub>S), m/z = 509 <i>S-Methyl lurasidone</i></p>

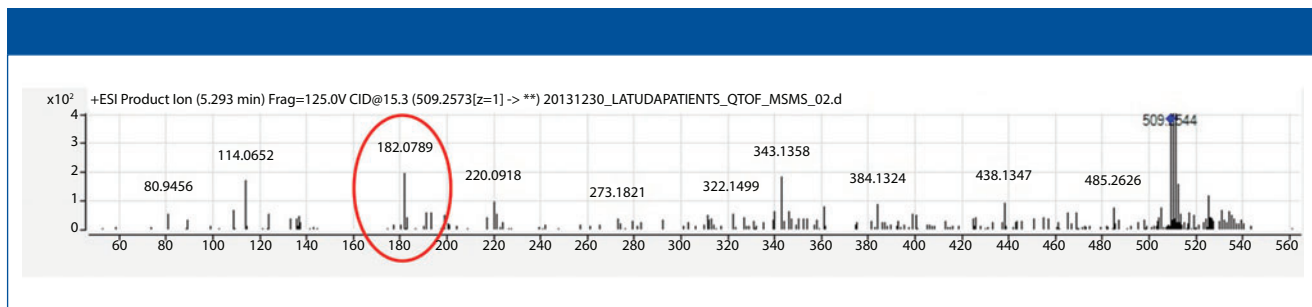


**Figure 1:** Fragmentation data from sample 8 Identified M8-M9-M10 Peak.

Lurasidone is metabolized in the liver primarily by CYP3A4. Metabolism includes oxidative N-dealkylation, hydroxylation of the norborane ring, S-oxidation, and reductive cleavage of the isothiazole ring, followed by S-methylation. Nearly two dozen metabolites of lurasidone have been previously identified, and only ~9% of the dose is excreted in urine (17–20). Typically, adherence to lurasidone therapy is monitored by evaluating levels of lurasidone and M11/ID-20219 (one of its metabolites) that were each predicted to be present in urine at approximately 12 and 24%, respectively. The structures for lurasidone and many of the confirmed metabolite structures can be seen in Table I.

Previously, we reported the identification of novel metabolites for monitoring aripiprazole, brexpiprazole, haloperidol, and quetiapine in urine that were not originally predicted (9–12). Because there are some similarities of these antipsychotics to lurasidone, we decided to determine if the urinary lurasidone compound(s) predicted from plasma studies were indeed the most abundant prior to development of a confirmation method. This work reports the identification of lurasidone and prevalent lurasidone metabolites in urine using LC–HRMS from patients prescribed lurasidone. Additionally, confirmation of the most prominent metabolites was tested in a validated, targeted, quantitative liquid chromatography–tandem mass spectrometry method (LC–MS/MS), which are at odds with current reports of urine metabolites (17–20).

## Experimental

### Chemicals

Lurasidone, lurasidone- $d_8$ , and hydrocodone- $d_6$  were purchased from Cerilliant (Round Rock, Texas). Hydroxylurasidone was a custom synthesis product purchased

from  $^{13}\text{C}$  Molecular (Greensboro, North Carolina). All solvents, including methanol (optima grade), formic acid (88%), acetonitrile (optima grade), ammonium acetate (optima grade), and isopropanol (optima grade), were purchased from VWR (Radnor, Pennsylvania, USA). Drug-free human urine was acquired from UTAK Laboratories (Valencia, California). Standards for S-methyl lurasidone and S-methyl hydroxylurasidone were not commercially available, and synthesis requests were unsuccessful.

### Sample Sets

Identification of lurasidone metabolites using LC–HRMS was completed on 13 authentic urine samples from patients who were prescribed the medication. After metabolite identification was complete, an LC–MS/MS confirmation was validated. An additional 56 patients were prescribed lurasidone at different doses, with specimens collected over three separate days for each patient used to confirm the accuracy of the method. These samples were provided voluntarily, and anonymously, to assist with the development of a lurasidone confirmation method. No identifying or demographic information was collected on these volunteers, other than the prescribed lurasidone dose. There was an alphanumeric code from the clinic that was provided to track the patients who provided samples over the course of the three separate days. None of the results were shared with the clinician to assist with treatment. Ameritox is accredited by the College of American Pathologists (CAP) and abides by CAP, Clinical Laboratory Improvement Amendments (CLIA), and Health Insurance Portability and Accountability Act (HIPAA) requirements. Due to the secondary analysis nature of this work and the absence of clinical conclusions,

neither the United States Food and Drug Administration (FDA) nor other clinical trial review or approval was obtained by Ameritox. Writing this manuscript did not involve human subjects, as defined by the U.S. Code of Federal Regulations (45 *CFR* 46.102); thus, an Institutional Review Board (IRB) approval of these specific research activities was unnecessary.

### LC–HRMS Sample

#### Preparation and Analysis

Thirteen patient urine specimens (100  $\mu\text{L}$ ) were diluted 5X with 400  $\mu\text{L}$  of a reference standard, (0.25  $\mu\text{g}/\text{mL}$  of hydrocodone- $d_6$  in water). Hydrocodone- $d_6$  was used as an internal reference standard for all LC–HRMS injections, to guarantee successful injection of the sample, and provide a retention time marker. Prepared samples were injected (5  $\mu\text{L}$ ) and separated on a Phenomenex Kinetex Phenyl-Hexyl, 2.1 x 50-mm, 2.6- $\mu\text{m}$  column (Torrance, California) at 50  $^{\circ}\text{C}$ , and analyzed on an Agilent 6530 Q-TOF (quadrupole time-of-flight mass spectrometer) with an Agilent 1290 LC system (Santa Clara, California). The LC–QTOF method conditions are detailed in a previous publication (12). A lurasidone control in drug-free urine (75 ng/mL) was run, along with the patient samples, to assist in positive identification of the parent compound, if present. No other standards were available or purchased to assist in identification, until a confirmation method was developed. Each sample was injected and analyzed twice.

The MS-only data were processed using Agilent Mass Hunter Qualitative Analysis and PCDL (Personal Compound Database and Library) manager software. A database of lurasidone and 11 of its possible metabolites' chemical formulas (Table I) was compiled, and used to search against the samples. The software matched com-

**Table II: Multiple reaction monitoring (MRM) mode transitions and mass spectrometry (MS) parameters**

Analyte	Transition*	Cone Voltage (v)	Collision Energy (v)	Dwell Time (s)
Lurasidone	493.5432 → 166.1404	74	40	0.039
	493.5432 → 177.1344	74	38	0.039
Hydroxylurasidone	509.6657 → 177.1191	52	44	0.039
	509.6657 → 182.13	52	46	0.039
S-methyl lurasidone	509.7 → 166.1404	52	44	0.039
	509.7 → 177.1191	74	40	0.039
S-methyl hydroxylurasidone	525.7 → 177.1191	52	44	0.039
	525.7 → 182.13	52	46	0.039
Lurasidone-d8	501.5287 → 120.0698	60	56	0.039
	501.5287 → 166.1375	60	42	0.039

\* For each analyte, the first transition is the quantification transition and the second transition is the qualification transition

pounds based on retention time (if available), mass ( $\pm 20$  parts per million or ppm), the isotopic distribution pattern, and the isotopic spacing theoretically derived from the chemical formula. To be identified as positive and a potential lurasidone metab-

olite, a compound had to have consistent retention times across multiple patient samples when a known retention time was lacking; otherwise, the retention times had to be within  $\pm 0.05$  minutes of a control. The mass accuracy had to be within  $\pm 20$

ppm; and the composite score of the mass accuracy and isotopic features had to be  $\geq 70$  (out of a possible 100). Compounds that had the highest area counts were also ranked and noted as the most abundant. To assist with differentiation of struc-

INTRODUCING THE NEW

## EXP<sup>2</sup> Ti-LOK™ AIO Fitting

- > Hand-Tight
- > All-In-One titanium-PEEK design
- > Featuring a permanently fixed driver
- > Compatible with all tubing types
- > Rated to 18,000+ psi



**optimize**technologies  
INNOVATIVE HPLC, UHPLC & LC/MS PRODUCTS

www.optimizech.com

Booth 700

American Society for Mass Spectrometry  
67th Conference | June 2-9, 2019 | Atlanta, GA



**Table III: High resolution mass spectrometry metabolite identification results**

Analyte (Molecular Weight)		Lurasidone (492.2559)	M8-M9-M10 (508.2508)	M11 (305.1627)	M11 Glucuronide (481.1948)	ID-20221 (524.2457)	ID-20222 (540.2406)	M22 (524.2821)	M21 (508.2872)	M4-M5-M6 (321.1576)
Subject ID	Run									
Subject 1	1		*					*	*	
	2		*					*	*	
Subject 2	1		*					*	*	
	2		*					*	*	
Subject 3	1	*						*	*	
	2	*						*	*	
Subject 4	1		*	*				*		
	2		*	*				*		
Subject 5	1		*					*	*	
	2		*					*	*	
Subject 6	1		*					*	*	
	2		*					*	*	
Subject 7	1		*					*		*
	2		*					*		*
Subject 8	1		*					*	*	
	2		*					*	*	
Subject 9	1	*						*	*	
	2	*						*	*	
Subject 10	1		*					*	*	
	2		*					*	*	
Subject 12	1	*						*	*	
	2	*						*	*	
Subject 13	1		*					*	*	
	2		*					*	*	

Green: Highly confident identification,  $\geq 90$  score; Yellow: Moderately confident identification,  $\geq 70$  but  $< 90$  score  
\* indicates top three most abundant, by peak area count, in each replicate.

A blank square indicates no identification was made or the identification was poorly identified,  $< 70$  score.

**Table IV: LC-MS/MS validation results**

	Linearity*			Carryover† Avg. Conc. (ng/mL) (n = 5)	Precision and Accuracy‡						Matrix§ % Matrix Effect	Interference Interfering compounds
	LOQ/ LOD (ng/mL)	ULOL (ng/mL)	$R^2$		Avg. % Target (n = 30)			Avg. % CV (n = 0)				
					200 ng/mL	500 ng/mL	3000 ng/mL	200 ng/mL	500 ng/mL	3000 ng/mL		
Lurasidone	5	5,000	0.9992	0.0	92.1	94.4	92.9	3.5	4.2	4.4	-11.00	None
Hydroxylurasidone	5	5,000	0.9996	0.0	99.6	104.0	100.2	4.3	3.3	2.8	4.30	None

\* The linearity results are compiled for all curve points and points that are between curve points, including 5, 10, 25, 50, 100, 250, 500, 1,000, 2,500, and 5,000 ng/mL, each run five times.

† Carryover was tested by running a matrix blank immediately following the ULOL.

‡ Precision and accuracy statistics were calculated by data from three separate concentration standards including 200, 500, and 3,000 ng/mL, 10 replicates each, prepared and run on 3 separate days.

§ Matrix data were calculated by dissolving the standards in normal human normal urine compared with a 'neat' preparation in chromatographic starting conditions (90% 2 mM ammonium acetate + 0.1% formic acid: 10% methanol).

tural isomers, such as M8/M9 and M10, fragmentation spectra were obtained and reviewed to identify which isomer was present at an identified metabolite peak, as needed.

#### LC-MS/MS Sample Preparation and Analysis

Hydroxylurasidone was received as a neat solid that was dissolved into methanol at a concentration of 1 mg/mL, and lurasidone

was received as a 100 µg/mL methanolic standard. Hydroxylurasidone and lurasidone were combined and diluted into a methanolic stock that was then further diluted into normal, drug-free human urine,

**Table V:** Prescribed lurasidone patient results from LC–MS/MS quantitative method

Compound	Statistics	Prescribed lurasidone dose					
		20 mg/day	40 mg/day	60 mg/day	80 mg/day	100 mg/day	120 mg/day
Lurasidone	Number of patients	19	12	2	15	1	6
	<i>n</i> *	50	33	6	45	3	16
	Minimum concentration (ng/mL)	5.7	7.2	15.6	10.1	62.5	12.4
	Median Concentration (ng/mL)	12.5	33.1	31.1	70	64.5	73.6
	Average concentration (ng/mL)	18.4	44.2	30.3	120.3	74	95.4
	Maximum concentration (ng/mL)	149	192.1	50.5	556.6	94.9	260.1
	Number of tests < LOQ	7	3	0	3	0	0
	% Positive	86%	91%	100%	93%	100%	100%
Hydroxylurasidone	Number of patients	19	12	2	15	1	6
	<i>n</i> *	50	33	6	45	3	16
	Minimum concentration (ng/mL)	6.1	5.2	6.3	11.8	153.9	7.8
	Median concentration (ng/mL)	22.9	50.9	40.8	146.8	186.4	146.3
	Average concentration (ng/mL)	43.7	91.9	43.6	220.3	176.2	171.2
	Maximum concentration (ng/mL)	456.1	586.5	93.5	897.1	188.4	586.3
	Number of tests < LOQ	5	1	0	3	0	0
	% Positive	90%	97%	100%	93%	100%	100%
S-Methyl lurasidone (M21)**	Number of patients	19	12	2	15	1	6
	<i>n</i> *	50	33	6	45	3	16
	Minimum concentration (ng/mL)	11	31.5	31.9	29	1032.3	81.6
	Median concentration (ng/mL)	60.6	252.6	186.4	1014.4	1404.7	607.6
	Average concentration (ng/mL)	102.4	407.5	185.4	1835.6	1345.5	1250.6
	Maximum concentration (ng/mL)	637.9	2766	324	9603.9	1599.4	6580.7
	Number of tests < LOQ	0	0	0	2	0	0
	% Positive	100%	100%	100%	96%	100%	100%
S-Methyl hydroxylurasidone (M22)	Number of patients	19	12	2	15	1	6
	<i>n</i> *	50	33	6	45	3	16
	Minimum concentration (ng/mL)	5.3	11.5	19.2	15.1	253.8	50.4
	Median concentration (ng/mL)	34.3	136.3	142.4	736.5	271.2	327.7
	Average concentration (ng/mL)	61	306.1	149.3	1026.9	327.2	853.9
	Maximum concentration (ng/mL)	365.9	2285.4	266.7	6401.5	456.6	4807.4
	Number of tests < LOQ	3	0	0	2	0	0
	% Positive	94%	100%	100%	96%	100%	100%

\**n* represents the number of patients times the three separate collection days for each patient as a total number of tests performed. Any specimen that failed to meet specimen validity requirements (specific gravity, pH, creatinine) is excluded from the total number of tests.

\*\*Concentrations for S-methyl lurasidone and S-methyl hydroxylurasidone are estimated from the lurasidone calibration curve.

to reach the appropriate calibrator (5, 25, 100, 500, and 1000 ng/mL) and quality control levels (75 ng/mL). Lurasidone-d8, 1 mg/mL methanolic stock, was diluted to 900 ng/mL in 0.1% formic acid in water solution. A 100  $\mu$ L aliquot of the sample (patient sample, calibrator, or quality control stock) and 400  $\mu$ L of lurasidone-d8 internal standard in 0.1% formic acid were added to a vial. Vials were then capped and vortexed for 10 s prior to injection of 5  $\mu$ L.

Samples were analyzed by LC-MS/MS on a Waters Acquity UPLC Xevo TQ-MS system (Waters Corporation, Milford, Massachusetts), a Waters Acquity UPLC CSH Phenyl-Hexyl 2.1 x 50-mm, 1.7- $\mu$ m UPLC column. The LC method and MS conditions can be found in Strickland and associates (12). Analyte transitions are listed in Table II. The acquisition method was run in dynamic multiple reaction monitoring (MRM) mode, in order to maximize the number of points across the various analyte peaks. The validation of this method followed CAP and CLIA guidelines (21–25), and an internal SOP (standard operating procedure) that has been described in detail elsewhere (26). It should be noted that, due to the lack of standards for S-methyl lurasidone and S-methyl hydroxylurasidone, they were unable to be validated, and estimates of their concentration were made by comparing the quantitative peak area ratio to the lurasidone calibration curve. These compounds were included as a proof of concept, to show their estimated prevalence and relative importance for lurasidone compliance in UDT for when standards might be available. Also, due to the lack of standards, the transition parameters were estimated from hydroxylurasidone and are not optimized.

## Results

The metabolite identification from the 13 patients analyzed by LC-QTOF can be seen in Table III. Compounds identified with the highest confidence (>90%) are highlighted in green, while less confident (>70% but <90%) compounds are highlighted in yellow. The three most abundant compounds for each specimen and replicate are noted with a star-asterisk in the respective square. For unidentified or not confidently identified compounds (<70%) for a given specimen replicate, the field is blank. It is clear that, although lurasidone was identified in almost all of the samples, it was not

consistently among the most abundantly identified compounds. Metabolite M11, the predicted major metabolite, was rarely confidently detected in these samples. Instead of lurasidone and M11, metabolites M21 (S-methyl lurasidone), M22 (S-methyl hydroxylurasidone), and isomer M8/M9 (hydroxylurasidone), or isomer M10 (lurasidone sulfoxide), were frequently detected. To determine whether hydroxylurasidone or the lurasidone sulfoxide (isomers) was present, the collected fragmentation data from the QTOF were analyzed, and are shown in Figure 1. The identification of a peak at  $m/z$  182 (red circle in Figure 1) confirmed the isomer as hydroxylurasidone by indicating a fragmentation of the hydroxylated norborane ring. If the identity was the lurasidone sulfoxide, expected fragmentation peaks of  $m/z$  152 or 237 from the oxidized sulfur atom on the isothiazole ring structure would be present. Additionally, the unhydroxylated norborane ring would have an expected  $m/z$  of 166. The absence of those expected peaks ( $m/z$  152, 237, and 166) in the spectra confirms the identity of the metabolite as hydroxylurasidone, and a custom synthesis of the molecule was requested to validate a confirmation method. S-methyl lurasidone and S-methyl hydroxylurasidone were also requested as custom synthesis products, but attempts to synthesize for the method were unsuccessful.

Upon receiving the hydroxylurasidone standard, an LC-MS/MS method was developed and validated. The results of validation of lurasidone and hydroxylurasidone are shown in Table IV. Although S-methyl lurasidone and S-methyl hydroxylurasidone were included in the method, without standards, validation was unable to be completed, and is the reason for their exclusion from Table IV. To ensure the ability to successfully detect and quantify lurasidone and hydroxylurasidone in patient specimens, samples from 56 additional patients (from three separate collection days) were provided for testing with the validated method. The results of these patient analyses are summarized in Table V, and separated by the prescribed dose. It is clear that testing for hydroxylurasidone helps with positive confirmation of taking lurasidone medication. It also appears, from the estimated concentrations of the S-methyl lurasidone and S-methyl hydroxylurasidone, that confirmation would be

easier with these metabolites, because they are more abundant than both lurasidone and hydroxylurasidone. However, the lack of standards for these compounds makes it impossible to currently validate a method for reporting UDT results for these compounds.

## Discussion

The advantages of HRMS analysis have been reviewed in the literature, including the extreme selectivity of such methods (10–12,27–30). Using this method, authentic urine samples of human subjects who were known to be taking chronic doses of lurasidone were tested for the presence of lurasidone and 11 possible metabolites. Due to the high mass resolving power and low mass error on the QTOF, compounds that have similar mass to charge ratios, but different chemical formulas, were differentiated with the searching algorithm (hydroxylurasidone and S-methyl lurasidone). Also, by eliminating extraction preparation methods, compound loss was mitigated. Using liquid as opposed to gas chromatography also helped ensure that compounds with low volatility can still be accurately analyzed. Surprisingly, neither of the predicted major urinary metabolites M5 nor M11 were found to be consistently excreted through human urine in large detectable amounts. This result could be due to the fact that M5 and M11 both have a carboxylic acid moiety that would be a possible glucuronidation target. This was considered, and the glucuronidated versions were searched for in patient samples and poorly identified. While this may indicate that the glucuronide metabolites of M5 and M11 are not present in urine in any appreciable amount, it could also be due to the poor ionizability of glucuronidated compounds. To confirm, an additional hydrolysis study could be completed to see if there is an increase in the prevalence of M5 and M11 in patients after hydrolysis. However, with the significant presence of hydroxylurasidone (M8/M9), S-methyl lurasidone (M21), and S-methyl hydroxylurasidone (M22), it seemed unnecessary to pursue hydrolysis as a means for analyzing for lurasidone compliance.

The presence of these metabolites in urine was not well predicted from results in blood. Hydroxylurasidone was estimated to have a prevalence of 2.8% as the M8 isomer,

and 0.4% as the M9 isomer; S-methyl lurasidone and S-methyl hydroxylurasidone were not predicted at any measurable amount (17–20). It does appear that the estimate of lurasidone at 12% might be reasonable, as all but one of the 13 patients in metabolite discovery had detectable amounts of the parent compound (17–20).

To better understand the relative amounts of each metabolite, lurasidone, hydroxylurasidone, S-methyl lurasidone, and S-methyl hydroxylurasidone present in urine, the results from the 56 patients used during method validation were analyzed. These results in Table V show that hydroxylurasidone, S-methyl lurasidone, and S-methyl hydroxylurasidone are present at approximately 2x, 7x, and 5x times, respectively, relative to lurasidone. All of the compounds show a general increase in concentration and percent positivity rate with increasing doses. It is clear that S-methyl lurasidone and S-methyl hydroxylurasidone provide slightly better positivity correlations at lower doses, but hydroxylurasidone does appear to provide enough benefit to help compensate for lower prevalence of lurasidone. Therefore, with the lack of available standards for S-methyl lurasidone and S-methyl hydroxylurasidone, hydroxylurasidone was validated to assist in UDT for lurasidone compliance.

## Conclusion

We successfully identified prevalent lurasidone metabolites in urine. Based on those identifications, we successfully validated a method for the purpose of UDT monitoring of lurasidone. The hydroxylurasidone metabolite provides benefit for lurasidone UDT monitoring by being more prevalent in the urine than lurasidone by ~2x, and providing more consistent positivity correlation at lower lurasidone doses. Although other metabolites are present in the urine in large concentrations, standards for those compounds are not available at this time. However, the proof-of-concept work with S-methyl lurasidone and S-methyl hydroxylurasidone shows that they are ~5x and ~7x greater in abundance than lurasidone, respectively, and would provide even better positivity correlation at low doses.

## References

- (1) M. Ko, and T. Smith, Urine Drug Monitoring in Patients on Prescribed Antipsychotic Medications. 29th Annual US Psychiatric and Mental Health Congress Oct 21–24 ([http://www.ingenuityhealth.com/wp-content/uploads/2016/11/Mental\\_Health\\_Populations\\_Study\\_US\\_Psych\\_2016\\_Poster.pdf](http://www.ingenuityhealth.com/wp-content/uploads/2016/11/Mental_Health_Populations_Study_US_Psych_2016_Poster.pdf)) (2016).
- (2) A.E. Cooper, P. Hanrahan, and D.J. Luchins, *Drug Benefit Trends* **15**(8), 34 (2003).
- (3) C.R. Dolder, J.P. Lacro, L.B. Dunn, and D.V. Jeste, *Am. J. Psychiatry* **159**, 103 (2002).
- (4) S. Offord, J. Lin, D. Mirski, and B. Wong, *Adv. Ther.* **30**(3), 286 (2013).
- (5) D.I. Velligan, F. Lam, L. Ereshefsky, and A.L. Miller, *Psychiatr. Serv.* **54**, 665 (2003).
- (6) D.I. Velligan, Y-W. F. Lam, D.C. Glahn, J.A. Barrett, N.J. Maples, L. Ereshefsky, and A.L. Miller, *Schizophr. Bull.* **32**(4), 724–742 (2006).
- (7) D.I. Velligan and P.J. Weiden, *Psychiatr. Times* **23**(9), 1–2 (2006).
- (8) R.A. Millet, P. Woster, M. Ko, M. DeGeorge, and T. Smith, Adherence to Treatment with Antipsychotic Medications Among Patients with Schizophrenia, Major Depressive Disorder, or Bipolar Disorder. Poster Presentation. (US Psychiatric and Mental Health Congress (USPMHC) San Diego, CA, 2015).
- (9) J. McEvoy, R.A. Millet, K. Dretchen, A.A. Morris, M.J. Corwin, and P. Buckley, *Psychopharmacology* **231**(23), 4421–4428 (2014).
- (10) J.R. Enders, S.G. Reddy, E.C. Strickland, and G.L. McIntire, *Clin. Mass. Spec.* **6**, 21–24 (2017).
- (11) O.T. Cummings, E.C. Strickland, J.R. Enders, and G.L. McIntire, *J. Anal. Toxicol.* **42**(4), 214–219 (2017).
- (12) E.C. Strickland, O.T. Cummings, A.A. Morris, A. Clinkscales, and G.L. McIntire, *J. Anal. Toxicol.* **40**(8), 687–693 (2016).
- (13) M.P. Cruz, *Drug Forecast* **36**(8), 489–492 (2011).
- (14) S. Caccia, L. Pasina, and A. Nobili, *Neuropsychiatric Disease and Treatment*, **2012**(8), 155–168 (2012).
- (15) R. Franklin, S. Zorowitz, A.K. Corse, A.S. Widge, and T. Deckersbach, *Neuropsychiatr. Dis. Treat.* **2015**(11), 2143–2152 (2015).
- (16) M. Ostacher, D. Ng-Mak, P. Patel, D. Ntais, M. Schlueter, and A. Loebel, *The World Journal of Biological Psychiatry*, **19**(8), 1–16 (2017). <http://doi.org/10.1080/15622975.2017.1285050> (2017).
- (17) Product Information: LATUDA oral tablets, lurasidone hydrochloride oral tablets. Sunovion Pharmaceuticals Inc. Marlborough, MA (2018).
- (18) R.C. Baselt, *Disposition of Toxic Drugs and Chemicals in Man* (Biomedical Publications, Seal Beach, CA, 11th Ed., 2010), pp 1232–1233.
- (19) Sunovion Pharmaceuticals Inc. Center for Drug Evaluation and Research Approval Package (Lurasidone). [https://www.accessdata.fda.gov/drugsatfda\\_docs/nda/2013/200603Orig1s010.pdf](https://www.accessdata.fda.gov/drugsatfda_docs/nda/2013/200603Orig1s010.pdf), Accessed May 8, 2018.
- (20) T. Ishibashi, T. Horisawa, K. Tokuda, T. Ishiyama, M. Ogasa, R. Tagashira, K. Matsu-moto, H. Nishikawa, Y. Ueda, S. Toma, H. Oki, N. Tanno, I. Saji, A. Ito, Y. Ohno, and M. Nakamura, *J. Pharmacol. Exp. Ther.* **334**(1), 171–181 (2010).
- (21) Association of Public Health Laboratories. CLIA-Compliant Analytical Method Validation Plan and Template for LRN-C Laboratories. December 2013.
- (22) F.T. Peters, O.H. Drummer, and F. Musshoff, *Forensic Sci. Int.* **165**, 216–224 (2007).
- (23) B. Levine, *Principles of Forensic Toxicology* (AACC Press, Washington, DC, 2nd edition 2003) pp 114–115.
- (24) U.S. Department of Health and Human Services, Food and Drug Administration. Guidance for Industry-Bioanalytical Method Validation (2001).
- (25) National Laboratory Certification Program (NLCP). Manual for Urine Laboratories. October 2010.
- (26) J.R. Enders and G.L. McIntire, *J. Anal. Toxicol.* **39**, 662–667 (2015).
- (27) J.M. Colby, K.L. Thoren, and K.L. Lynch, *J. Anal. Toxicol.* **42**(4), 201–213 (2018).
- (28) E. Partridge, S. Trobbiani, P. Stockham, T. Scott, and C.A. Kostakis, *J. Anal. Toxicol.* **42**(4), 220–231 (2018).
- (29) J.M. Colby, K.L. Thoren, and K.L. Lynch, *J. Anal. Toxicol.* **41**(1), 1–5 (2017).
- (30) S.K. Manier, A. Keller, J. Schaper, and M.R. Meyer, *Nature: Sci. Rep.* **9**(2741), 1–11 (2019).

**Erin C. Strickland** is with Ameritox, LLC, in Greensboro, North Carolina. **Jeffrey R. Enders** is with the Molecular Education, Technology and Research Innovation Center of North Carolina State University, in Raleigh, North Carolina. **Gregory L. McIntire** is with Premier Biotech, in Minneapolis, Minnesota. Direct correspondence to: [gregorymcintire2@gmail.com](mailto:gregorymcintire2@gmail.com)

# Quantitation and Nontargeted Identification of Pesticides in Spinach Extract with GC×GC–TOF-MS

Accurate detection, identification, and quantitation of compounds in high matrix food extracts often proves challenging, even to experienced analysts. This work becomes more challenging as regulatory agencies drive limits of detection (LODs) lower, while simultaneously increasing the number and types of compounds that must be targeted. Selected ion monitoring and tandem mass spectrometry (MS/MS) techniques can help mitigate matrix interferences, but they may not be selective enough for all compounds in the most challenging matrices. Furthermore, these types of targeted analysis techniques remove the possibility for retrospective nontargeted analysis of the data, preventing analysts from detecting new or emerging contaminants. In contrast, comprehensive two-dimensional gas chromatography (GC×GC) dramatically improves chromatographic resolution of analytes within a sample, often completely separating target compounds from would-be matrix interferences. Additionally, new time-of-flight mass spectrometers (TOF-MS) allow for full scan collection at selected ion monitoring (SIM)-level sensitivities, obviating the need for quadrupole-based systems. In this article, we demonstrate the use of GC×GC–TOF-MS as a methodology to combat matrix interferences, and quickly target and quantify suspected contaminants, while still allowing nontargeted analyte detection in a single sample injection.

**Todd Richards and Joseph Binkley**

The “quick, easy, cheap, effective, rugged, and safe” (QuEChERS) technique has become the predominant method to extract pesticides from a variety of food products (1). Since its introduction, many improvements have been made to the extraction chemistries, not only to improve pesticide recoveries, but also to decrease the amount of coextracted commodity matrix. Even so, particularly problematic matrices still exist. In the case of samples that contain high levels of fat (fish, avocados, and nuts) or pigmentation (spinach and blueberries), large amounts of unwanted matrix still pass into the final extract. These coextracted compounds often negatively affect pesticide detection and quantitation, challenging the efforts of analysts worldwide, especially as limits of detection (LODs) are decreased by numerous regulatory entities.

In most analyses, a mass spectrometer is coupled to a single dimension of chromatographic separation. In the case of high matrix commodities, the likelihood of coextracted interferences is high, and the system becomes dependent on complex mass transitions, their corresponding retention windows, and peak picking routines (deconvolution, if available) to do the heavy lifting of fully resolving and identifying the target analytes from the ubiquitous background signals. Furthermore, these selective sample data are collected in limited mass windows, and known to be completely ill-suited for nontargeted interrogation. To examine the samples for new or emerging contaminants, samples must be retained for future analyses on an independent analysis system capable of nontargeted work.

Alternatively, one could utilize the additional separation efficiency delivered by two-dimensional gas chromatography (GC×GC) to better chromatographically separate target analytes from matrix interferences and a mass spectrometer (such as time-of-flight [TOF]-MS) capable of collecting full scan data. These separations, combined with the full scan data at the sensitivity available with modern TOF-MS systems (low femtograms on column), allow for successful quantitation of target compounds, plus accurate identification of nontargeted analytes in a single injection.

In this article, we demonstrate improvement in experimental metrics (identification, limit of detection [LOD], and linearity) when performing both quantitative and nontargeted analysis with GC×GC-TOF-MS on spiked extracts from spinach, which is known to be a challenging food matrix.

### Experimental Design

Bagged spinach was purchased from a local grocery chain. Using a commercially available QuEChERS extraction kit (Restek PNs 25852 and 26225), a bulk QuEChERS extract was created, and subsequent dSPE cleanup of the spinach was performed. Following the kit instructions (1), 15 g of leaf spinach was homogenized, and combined with 15 mL of 1% acetic acid in acetonitrile in a 50 mL conical tipped tube. The contents of the prepared salt packet (6 g anhydrous  $\text{MgSO}_4$  and 1.5 g anhydrous  $\text{Na}_2\text{SO}_4$ ) were added, the tube immediately capped and then shaken, by hand, for 1 min. After shaking, the mixture was centrifuged for 5 min at 3500 RPM, separating the organic layer from the spinach solids, water, and unbound salts mixture. Post centrifugation, 6 mL of the organic layer was added to a dSPE tube containing 900 mg  $\text{MgSO}_4$ , 15 mg primary and secondary amine (PSA), and 45 mg graphitized carbon black (GCB). This second clean-up step is responsible for the primary removal of pigments (GCB), sugars, organic and fatty acids (PSA), and any remaining water ( $\text{MgSO}_4/\text{H}_2\text{O}$ ), though attention must be paid not to

overemploy these compounds, as they may also bind pesticides and lower recovery efficiencies. The dSPE tube was immediately capped, shaken for 2 min, and then centrifuged for 5 min at 3500 rpm. The supernatant was removed from the dSPE material by pipette, and stored in a clean, conical tipped tube. Extracts from duplicate, concurrent preparations were pooled, and centrifuged a final time. This final step is not specifically called for in the kit instructions, though we

have found it useful, because it helps ensure that any accidentally pipetted dSPE material is removed from the final extract.

From the pooled extract, a small aliquot was set aside, and the remainder used to create a series of nine matrix-matched quantitation standards, spiked at concentrations from 0.05 to 200 ng/g with a commercially available chlorinated pesticide mix (Restek PN 32564). Dilutions of the stock standard were made so the ratio

## SMART LABS CHOOSE ON-SITE GAS GENERATION



### $\text{H}_2$ , $\text{N}_2$ AND ZERO AIR ON-DEMAND

- Consistent Purity
- Consistent Pressure
- Proven Safe
- Cost Effective
- Eliminates Cylinder Storage and Delivery Issues



ASMS • June 2-6 • Atlanta, GA  
SEASR • June 12-14 • Atlanta, GA

**PROTON**<sup>®</sup>  
ON SITE

+1.203.949.8697

[www.ProtonOnSite.com](http://www.ProtonOnSite.com)

Table I: Analytical system data collection parameters	
Mass Spectrometer	LECO Pegasus BT 4D TOF-MS
Ion source temperature	250 °C
Mass range	45–570 m/z
Acquisition rate	280 spectra/sec (GC×GC) 8 spectra/sec (GC)
Gas chromatograph	LECO GCxGC Quad Jet Thermal Modulator
Injection	1- $\mu$ L splitless @ 250 °C
Carrier gas	Helium @ 1.4 mL/min, corrected constant flow.
Primary column	Rxi-5ms, 30-m x 0.25-mm i.d. x 0.25- $\mu$ m film (Restek, Bellefonte, PA, USA).
Secondary column	Rtx-200, 1-m x 0.25-mm i.d. x 0.25- $\mu$ m film (Restek, Bellefonte, PA, USA).
Temperature program	1 min at 75 °C, ramped 10.2 °C/min to 320 °C, held 8 min Secondary oven maintained +5 °C relative to primary oven
Modulation	2 s period, +15 °C relative to 2nd oven
Transfer line	330 °C

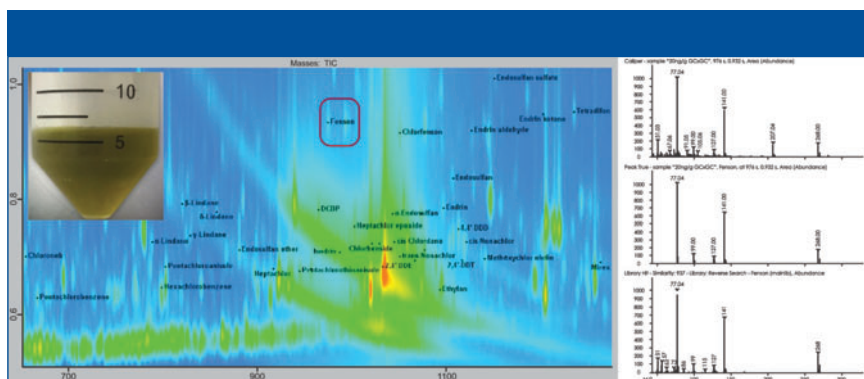


**Figure 1:** Section of contour plot for the spinach QuEChERS extract with dSPE cleanup (inset upper left), spiked with pesticides at 20 ng/g. In this example, the second dimension of separation effectively moved Fenson and other pesticides away from high concentration matrix interferences. The chromatographic separation of GC×GC significantly improves both analyte detection and quantitation.

of spiking standard (20  $\mu$ L) to matrix extract (180  $\mu$ L) was consistent in all the experimental standards. The chlorinated mix was chosen because it is less likely that any of the pesticides in this mix would already be present in the spinach, and thus bias the quantitation results. Data from both the matrix-matched standards and unspiked extract were collected in both traditional, single dimension GC as well as GC×GC modes, using conditions described in Table I. Target peak detection, identification, and quantitation limits for each analyte were determined following the criteria for unit mass resolution TOF-MS systems

as described in SANTE/11813/2017 (2). Table II shows a reproduction of Table 4 from SANTE/11813/2017, where these criteria are summarized. Following data collection, files were analyzed with ChromaTOF BT software, using both Target Analyte Find (TAF) for quantitative purposes and NonTarget Deconvolution (NTD) for qualitative investigation for incurred contaminants.

## Results and Discussion

### Quantitation and GC×GC Improvements

Figure 1 shows an example of data collected using a GC×GC–TOF-MS

system. In this plot, areas of increased signal are shown with increasing color intensity (red being the highest), and the location of individual pesticides are indicated with labels and peak markers (black dots). In this sample, it is demonstrated that many of the pesticides are chromatographically resolved from the much more abundant matrix background. Additionally, fenson is highlighted with a red box as an example, since it was effectively separated from a very large area of matrix.

With LC–MS experiments, it is well known that high levels of matrix tend to suppress target compound ionization (3), leading to various challenges. In GC–MS experiments, the matrix poses its own set of hurdles, as the matrix tends to interfere by adding spurious signals, sometimes referred to paradoxically as *signal enhancement*. Far from improving the target signal, matrix noise may skew the lower ends of quantitation curves, or unequally affect ion ratio masses. If, by chromatography, one can separate these targeted compounds from the matrix, interference effects are properly mitigated before detection by the mass spectrometer. As a result, effects on targeted signals are decreased, leading to improvements in LODs and quantitation linearity. As one will see, these improvements are entirely due to both the effect of the thermal modulation process, and secondary chromatographic separation when performing GC×GC.

Figures 2 and 3 show examples of calibration curves comparing GC to GC×GC data for the compounds chloroneb, mirex, and chlorbenzide. When examining the curves in Figure 2, one can see a significant decrease in LOD (factor of 10x) by using GC×GC with nearly equivalent linearity. Also worth noting is the range of the calibration curves. The entire dynamic range has shifted to lower concentrations. The improvements in the calibration curves and LODs for these analytes are due to both the increased selectivity

**Table II:** A reproduction of Table 4 from SANTE /11813/2017 describing peak identification requirements. The highlighted sections apply to Pegasus BT 4D, single dimension GC and GC×GC data.

MS Detector Characteristics		Acquisition	Requirements for Identification	
Resolution	Typical systems (examples)		Minimum number of ions	Other
Unit mass resolution	Single MS	Full scan, limited m/z range, SIM	3 ions	S/N ≥ 3 (d) Analyte peaks from both product ions in the extracted ion chromatograms must fully overlap.
	Quadrupole, ion trap, TOF			
Accurate mass measurement	MS/MS	Selected or multiple reaction monitoring (SRM, MRM), mass resolution for precursor-ion isolation equal to or better than unit mass resolution	2 product ions	Ion ratio from sample extracts should be within ±30% (relative) of average of calibration standards from same sequence
	Triple quadrupole, ion trap, Q-trap, Q-TOF, Q-Orbitrap			
	High Resolution MS: (Q)-TOF (Q)-Orbitrap FT-ICR-MS Sector MS	Full scan, limited m/z range, SIM, fragmentation with or without precursor-ion selection, or combinations thereof	2 ions with mass accuracy ≤ 5ppm (a, b, c)	S/N ≥ 3 (d) Analyte peaks from precursor and/or product ion(s) in the extracted ion chromatograms must fully overlap  Ion ratios: see D12

a) Preferably including the molecular ion, (de)protonated molecule or adduct ion  
 b) Including at least one fragment ion  
 c)  $l_s < 1$  mDa for  $m/z < 200$   
 d) In case noise is absent, a signal should be present in at least 5 subsequent scans

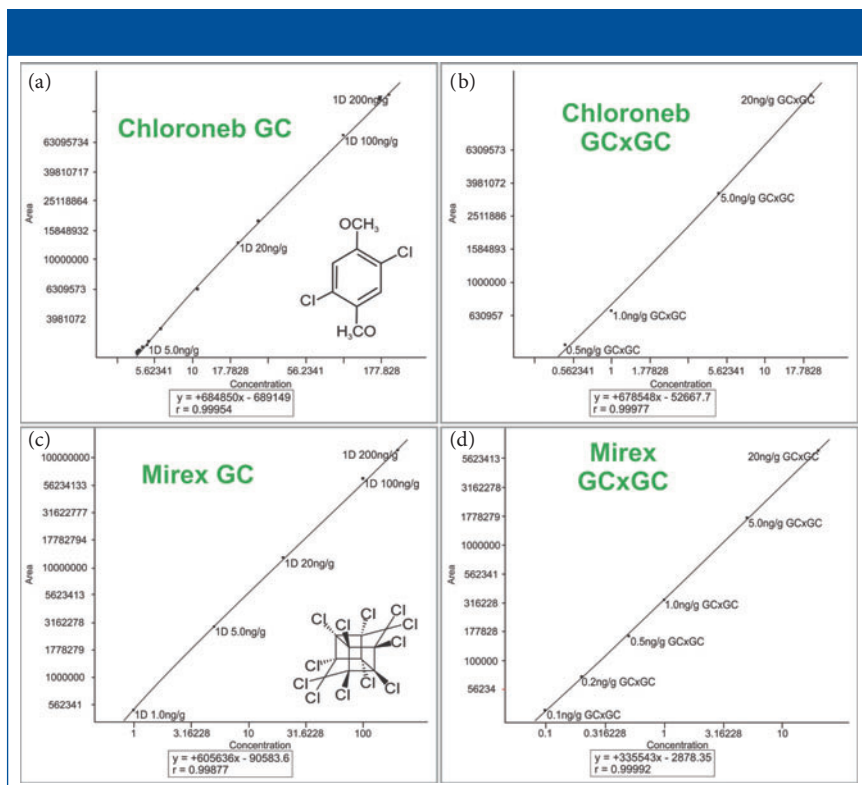


**Figure 2:** Example GC and GC×GC quantitation curves. The axes are scaled logarithmically for better visualization of the low concentration section of each curve. Shown in the figure are: (a) chloroneb by GC, (b) chloroneb by GC×GC, (c) mirex by GC, and (d) mirex by GC×GC.

from enhanced chromatographic resolution, and the improved sensitivity afforded by cryogenic zone compression in GC×GC. In the left

side of Figure 3, chlorbenside has very significant matrix coelution in the first dimension ( $x$  axis). The calibration curve is improved dra-

matically by the chromatographic separation of compounds (specifically the second dimension retention time) versus separation by mass only with one-dimensional GC systems. For GC×GC-TOF-MS systems, it is the separation of mass combined with the separation of time (chromatographic) that leads to these advantages. The advantages of the technique become very distinct, as shown in the right side of Figure 3, where the linearity is improved (note the quadratic fit on the simple GC experiment) as well as the limit of detection. Note further that the matrix interference for chlorbenside contains isobaric co-elutions, which would limit quantitation with techniques using GC with quadrupole MS. This trend is further illustrated in Table III, which shows marked improvement in LOD and linearity for GC×GC data compared to the single dimension separation for a variety of spiked pesticides.

**Nontargeted Analysis and Identification**

In Figure 4, one can observe standard deconvolution results comparing GC and GC×GC data. Mathematical identification of true signal components

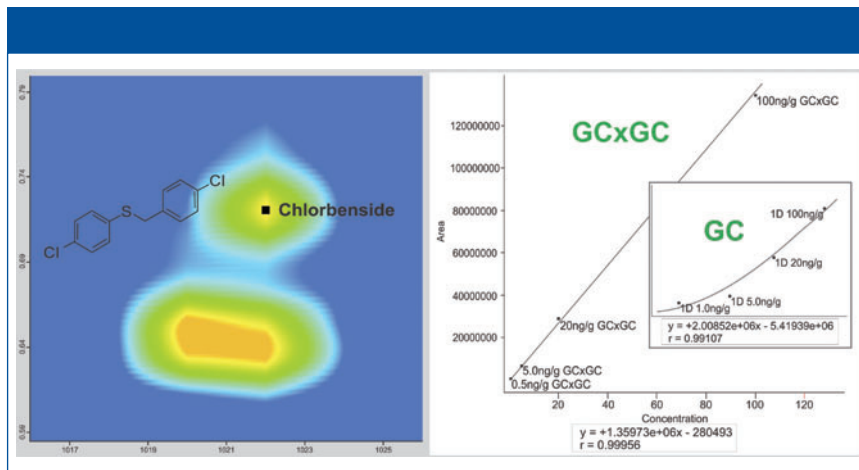


**Figure 3:** GC×GC resolution of chlorbenside from the matrix interference. The GC×GC separation allows for a linear and sensitive quantitation curve. In the traditional, single-dimension GC separation the coeluting matrix completely obscures the pesticide below 20 ng/g making consistent, accurate integration impossible.

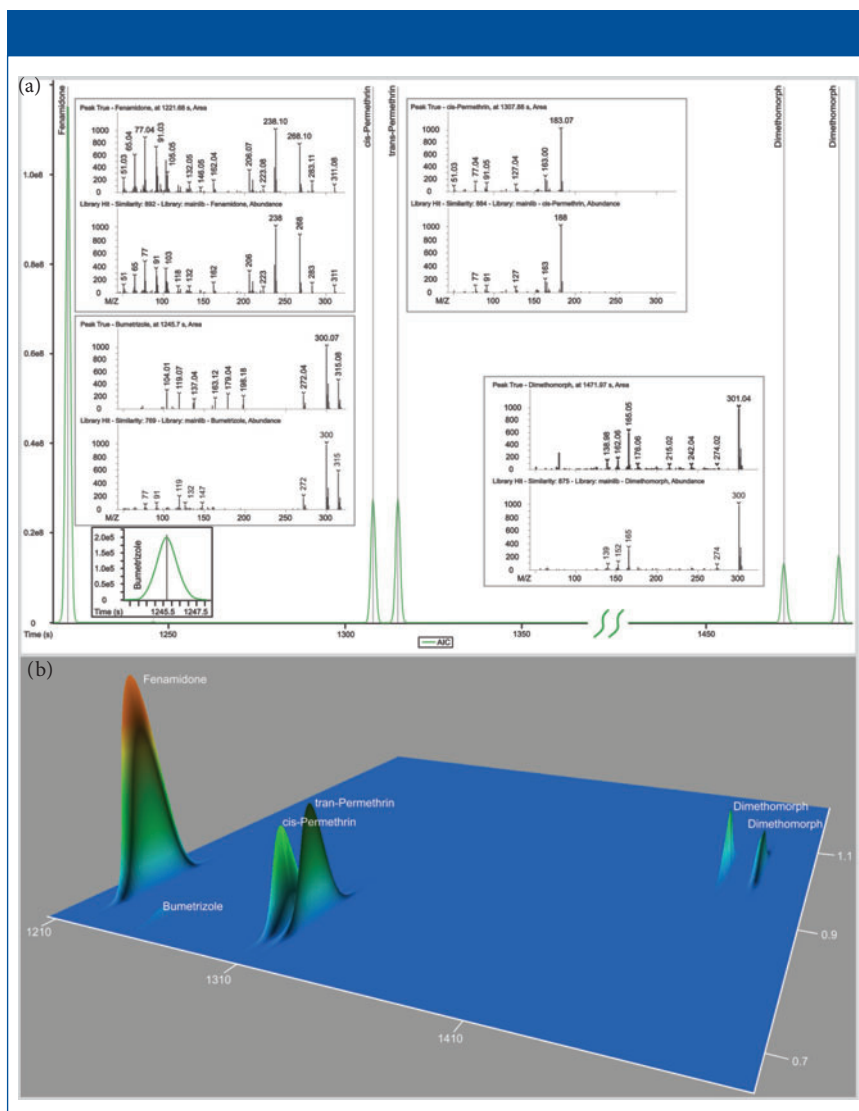


**Figure 4:** Initially identified incurred pesticides and ultraviolet (UV) stabilizer (Bumetrizole) shown as both (a) traditional GC chromatogram and (b) GC×GC surface plot.

over noise and GC co-elutions are handled with the NonTarget Deconvolution algorithm provided by Chroma-TOF for Pegasus BT. The identification of these known components was performed by comparison of the deconvoluted spectra to the spectra in the NIST GC–MS library (2017). The initial result lead us to several pesticides and an ultraviolet (UV) stabilizer in both the traditional GC and GC×GC data files (Figure 4). However, in the figure, there is no distinct difference between the capabilities of GC and GC×GC in these cases, since the components are well resolved in the primary GC dimension. Perfect co-elutions do frequently exist in nontargeted analysis of complex matrices, and are beyond the capabilities of mathematical deconvolution. These situations benefit greatly from the use of GC×GC.

Figures 5 and 6 show an example of the advantages of GC×GC for nontargeted analysis. Review of the GC×GC data lead to the discovery of an unexpected pesticide, chlorantraniliprole, that was not readily apparent in the single dimension GC data. In the GC×GC contour plot (left) of Figure 5, the pesticide is cleanly resolved in the second dimension, whereas perfectly co-eluting with a matrix component in the first dimension. Contrast this result with Figure 6, where the compound was initially missed, due to a nearly perfect coelution with the abundant matrix compound. In Figure 6, the deconvoluted spectrum obtained from GC analysis is actually a combination of chlorantraniliprole and the interfering component resulting in an awful similarity score. The deconvoluted spectra of Figure 5 show the two compounds successfully separated chromatographically, leading to a clean spectrum and a high similarity score for chlorantraniliprole.

## Conclusion

High levels of matrix interference can directly affect the ability to accurately and reliably quantitate low levels of pesticides, and further hamper nontargeted workflows. This study was designed to evaluate and demonstrate the effectiveness of GC×GC separa-

**Table III:** Comparison of GC and GC×GC quantitation results for selected pesticides. A valid quantitation curve for chlorbenside below 20 ng/g was not possible with single dimension GC due to matrix interference which was chromatographically resolved with GC×GC as shown in Figure 3.

Analyte	GC LOD ng/g	GC Correlation Coefficient	GC×GC LOD ng/g	GC×GC Correlation Coefficient
Chloroneb	5.0	0.99954	0.5	0.99977
Pentachlorobenzene	0.2	0.99901	0.1	0.99997
Pentachloroanisole	0.2	0.99915	0.1	0.99966
Heptachlor	1.0	0.99813	0.5	0.99972
Aldrin	1.0	0.99920	0.2	0.99985
Heptachlor epoxide	1.0	0.99913	0.5	0.99982
Chlorbenside	Quantitation Not Possible		0.5	0.99956
Dieldrin	5.0	0.99870	1.0	0.99560
Tetradifon	5.0	0.99902	0.5	0.99997
Mirex	1.0	0.99877	0.1	0.99992

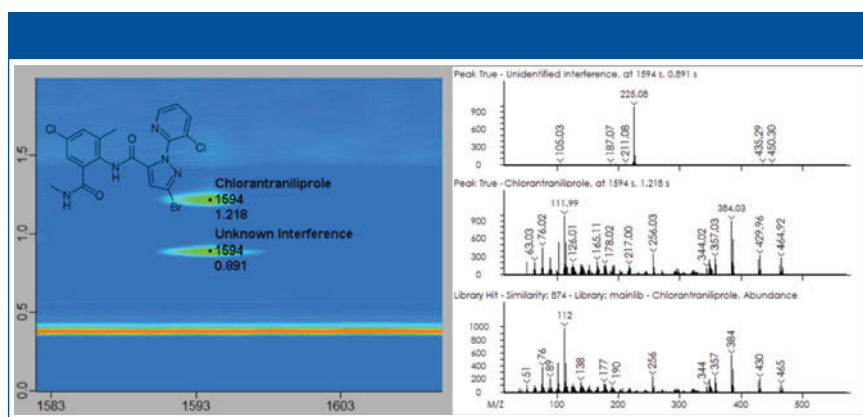


**Figure 5:** GC×GC contour and spectral plots of chlorantraniliprole and the interfering matrix compound. The two compound signals have been normalized to allow for easier viewing. Note the chromatographic separation from the column bleed (horizontal, orange band) and the improvement in the deconvolution of both compound spectra are compared to the traditional, single dimension GC separation results as shown in Figure 6.

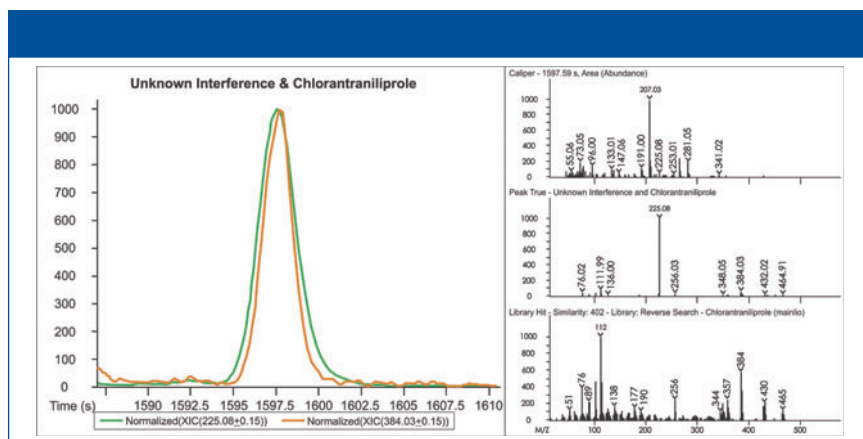


**Figure 6:** GC extracted ion chromatogram (XIC) and spectra plots of chlorantraniliprole (orange) and matrix (green). The two compound signals have been normalized to allow for easier viewing. The top, raw spectra plot shows the intensity of both compounds relative to the overriding column bleed signal. The GC–MS library spectrum for chlorantraniliprole (bottom) is shown for reference. In the middle deconvoluted spectra you can see the most prevalent ions from chlorantraniliprole although, they are obviously dwarfed by ions from the coeluting matrix compound.

tions to mitigate these matrix effects, compared to a traditional, single dimension separation for both targeted, quantitative and nontargeted, qualitative workflows. As shown in these examples, the additional level of chromatographic resolution achievable through GC×GC can indeed reduce matrix interferences, and improve the effectiveness of both types of analyses. By decreasing the level of matrix-induced noise, quantitation becomes both more accurate and more sensitive, leading to dramatic improvements in non-target peak detection, identification, and quantitation.

## References

- (1) M. Anastassiades, S.J. Lehotay, D. Stajnbaher, and F.J. Schenck, *J. AOAC International* **86**, 412 (2003).
- (2) European Commission: Directorate General For Health And Food Safety. SANTE/22813/2017, Guidance document on analytical quality control and method validation procedures for pesticide residues and analysis in food and feed. URL: [https://ec.europa.eu/food/sites/food/files/plant/docs/pesticides\\_mrl\\_guidelines\\_wrkdoc\\_2017-11813.pdf](https://ec.europa.eu/food/sites/food/files/plant/docs/pesticides_mrl_guidelines_wrkdoc_2017-11813.pdf).
- (3) T.M. Annesley, *Clin. Chem.* **49**(7) 1041–1044 (2003). DOI: 10.1373/49.7.1041

**Todd Richards** and **Joseph Binkley** are with LECO Corporation, in Saint Joseph, Michigan. Direct correspondence to: [todd\\_richards@leco.com](mailto:todd_richards@leco.com)

# High-Throughput Structure-Based Profiling and Annotation of Flavonoids

One of the most widely encountered challenges in untargeted metabolomics is how to identify and annotate unknown compounds. Many classes of compounds, such as flavonoids, endocannabinoids, steroids, and phospholipids, are difficult to confidently identify and annotate, due to their structural diversity and the limited availability of reference standards. This study applies a novel mass spectrometry-based flavonoid profiling workflow to characterize and structurally annotate a large number of unknown flavonoids in fruit juice and vegetable juice samples.

**Simon Cubbon**

**W**idely found in fruits and vegetables, as well as plant-derived products such as tea, cocoa, and wine, flavonoids are powerful antioxidants with anti-inflammatory and immune system benefits (1). With diverse and important biological roles, flavonoids have been the focus of much research interest.

Untargeted flavonoid profiling using high-resolution mass spectrometry (MS) is one of the most widely used approaches for flavonoid analysis, because the resulting data can provide insight into the biological functions and potential health benefits of these compounds. However, the comprehensive identification of flavonoids remains challenging, due to their structural diversity. Because flavonoids are involved in a broad range of secondary metabolic pathways that involve modifications such as acylation, hydroxylation, methylation, prenylation, and glycosylation, large numbers of isomeric and isobaric structures may exist in the same sample. Indeed, over 10,000 flavonoid structures have been isolated (2).

Despite the vast number of reported flavonoids, the limited availability of authentic flavonoid reference standards, and therefore reference spectra, means that many unknown flavonoid compounds encountered in profiling studies do not have an exact match in MS spectral libraries. This is particularly true for flavonoids with multiple glycoside modifications, which can be very challenging to characterize. Consequently, many flavonoid structural characterization studies published to date have involved the manual assignment of fragment ions generated from tandem mass spectrometry ( $MS^2$ ) and higher order MS data ( $MS^n$ ) (3,4). This painstaking analysis requires in-depth knowledge of

flavonoid fragmentation rules, and is both labor- and time-intensive. Moreover, for the majority of flavonoid glycoconjugates,  $MS^2$  does not generate sufficient diagnostic fragment ion information to annotate aglycone structures (5), or differentiate between isomers.

Multiple stage mass spectrometry can be used to systematically fragment analytes to generate more structurally relevant fragment ion information. This approach can be used to generate a so-called “spectral tree” to support the annotation of unknown compounds. Here, we report a novel structure-based flavonoid profiling workflow for the detection and identification of unknown flavonoids in fruit and vegetable juices. The method uses comprehensive fragment ion information generated from higher-energy collisional dissociation (HCD) and collisional induced dissociation (CID) Fourier transform (FT)  $MS^2$ , as well as higher order CID-FT- $MS^n$ , for rapid flavonoid annotation. We demonstrate this workflow for the annotation of flavonoid glycoconjugates, although the approach may be applied to other transformation products of secondary metabolism.

## Experimental Sample Preparation

Three commercially available fruit and vegetable juice samples (kale juice; berries juice mixture, consisting of apple, orange, cherry, peach, mango strawberry, and blackberry juices; and a “red” juice mixture, consisting of apple, strawberry, banana, beet, and raspberry juices) were analyzed in this study. Each juice sample was filtered and diluted two-fold with methanol prior to analysis.

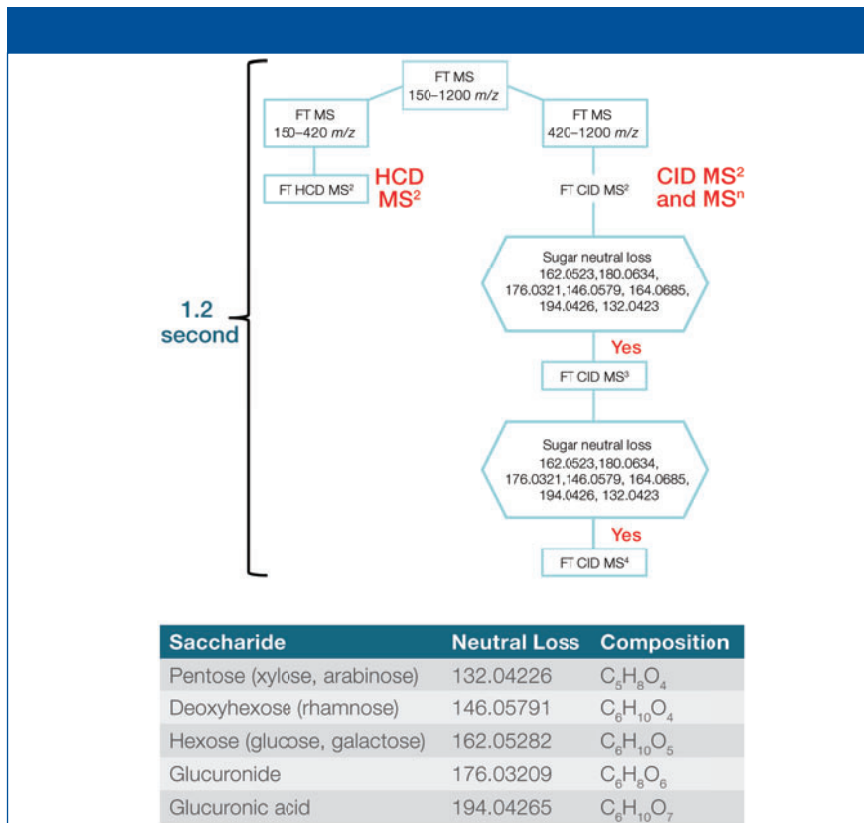


**Figure 1:** Flowchart visualizing the intelligent, automated product ion-dependent MS<sup>n</sup> method, and table detailing the targeted sugar neutral loss scheme.

**UHPLC Conditions**

Separations were performed on a Thermo Scientific Vanquish ultra-high-pressure liquid chromatography (UHPLC) system. The gradient was as follows: 0.5% to 10% B in 1 min, 10 to 30% B in 9 min, 30 to 50% B in 8 min, 50 to 99% B in 4 min, hold at 99% B for 3 min, 99 to 0.5% B in 4.99 min. Mobile phase A was water with 0.1% formic acid, and mobile phase B was methanol with 0.1% formic acid, operating at a flow rate of 200 μL/min. A Thermo Scientific Hypersil Gold (2.1 × 150 mm, 1.9 μm) column, operating at 45 °C, was employed. Each sample (2 μL injection volume) was analyzed in triplicate.

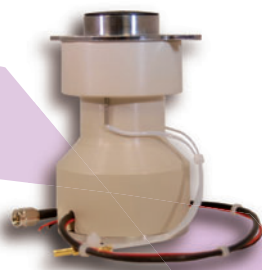
**MS Conditions and Spectral Tree Approach**

MS data were collected on a Thermo Scientific Orbitrap ID-X Tribrid mass spectrometer using electrospray ionization (ESI). A default acquisition template was used to collect the maximum amount of MS<sup>n</sup> spectral tree data to enable the structure annotation of



# PRECISE ANALYSIS

## for Clinical Mass Spectrometry



*Long-Life Bi-Polar Time of Flight Detectors*

Our unique optically coupled Bi-Polar TOF detectors offer stable gain and long lifetime even for the most demanding clinical mass spectrometry applications. Reduced instrument down time results in higher sample throughput and lower cost per sample.

Learn how our technology can refine your analysis. Visit us at **ASMS at booth #609** or at [www.photonis.com](http://www.photonis.com).

[www.photonis.com](http://www.photonis.com)

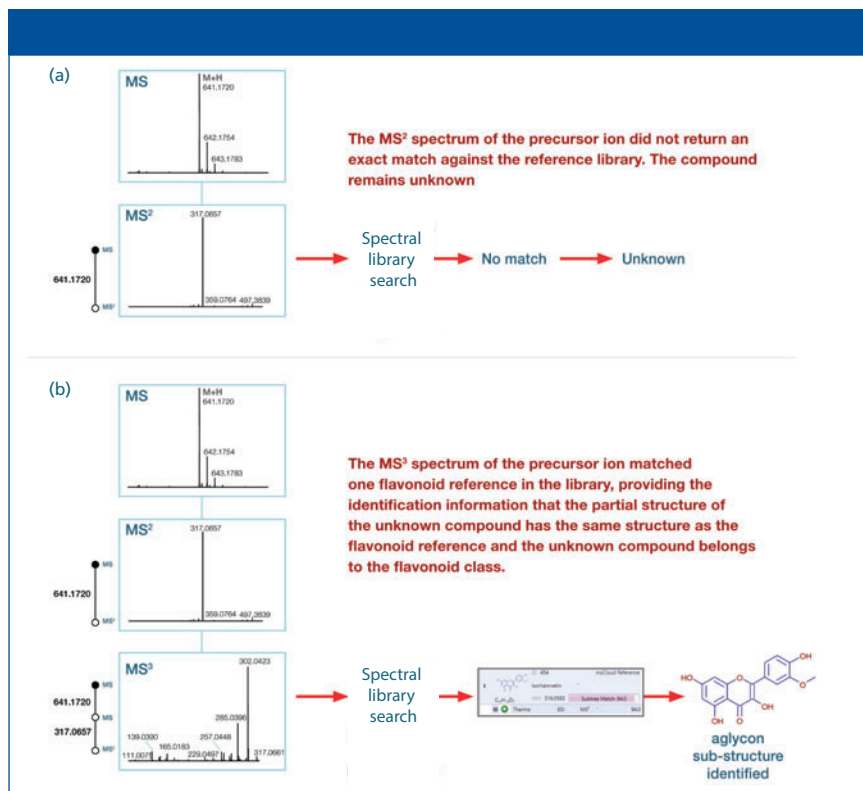


**Figure 2:** (a) MS<sup>2</sup> and (b) MS<sup>3</sup> spectral trees for an unknown compound (M + H: 641.1720) detected in the kale juice sample.



**Figure 3:** (a) An unknown flavonoid compound (MW = 742.23274) that matched both mass lists; (b) candidate structures proposed using the Arita Lab 6549 flavonoid structure database and the ChemSpider database for the identified compound.

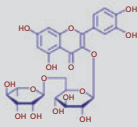
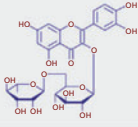
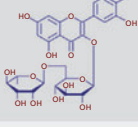
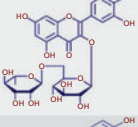
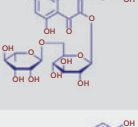
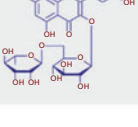
unknown flavonoid compounds. A short cycle time of 1.2 s was chosen to permit sufficient MS scan points across each peak for precise quantitation, while delivering high resolution spectral data. Because HCD MS<sup>2</sup> provides sufficient fragment ions for structure annotation when the flavonoid compounds do not have glycol modifications, only HCD MS<sup>2</sup> data were collected for precursor ions in the mass range 150–420 *m/z*. For precursor ions in the mass range 420–1200 *m/z*, glycol modifications were anticipated, and product ion-dependent MS<sup>n</sup> method was employed. This approach involved a high-resolution accurate mass (HRAM) full MS scan, followed by CID MS<sup>2</sup> scans. Product ions generated from each MS<sup>2</sup> scan were monitored by the mass spectrometer, and an MS<sup>3</sup> scan was triggered if one or more predefined neutral sugar losses were detected. An additional MS<sup>4</sup> scan was triggered if predefined neutral sugar losses were detected from the MS<sup>3</sup> scan. The product ion dependent method and predefined neutral sugar loss scheme are shown in Figure 1.

## Data Analysis

The collected MS<sup>n</sup> spectral tree data were initially processed using Thermo Scientific Mass Frontier 8.0 software to determine which compounds included the basic flavonoid structure. Detected flavonoid-related compounds were subsequently annotated using a flavonoid structure database and structural ranking tools within the Thermo Scientific Compound Discoverer 3.0 software.

## Results

The MS<sup>n</sup> approach described in the experimental section was used to systematically fragment flavonoids, generating spectral trees. A representative MS<sup>3</sup> spectral tree, generated from an unknown compound detected in the kale juice sample, is shown in Figure 2. The MS<sup>2</sup> spectrum for the precursor ion at *m/z* 641.1720 did not return an exact match against the cloud-based mass spectral database (mzCloud) spectral library (Figure 2a). However, fragmenting the MS<sup>2</sup> product ion present at *m/z*

Table I: Rutin and its secondary metabolites identified using MS <sup>2</sup> and MS <sup>n</sup> workflows			
Molecular Weight	ID Structure/Substructure in MF 8.0	Identified with MS <sup>2</sup> in CD 3.0	Identified with MS <sup>n</sup> and FiSh score in CD 3.0
610.1539	C <sub>27</sub> H <sub>30</sub> O <sub>16</sub> MW: 610.1534 	●	●
626.1490	C <sub>27</sub> H <sub>30</sub> O <sub>16</sub> MW: 610.1534 	✗	●
756.2120	C <sub>27</sub> H <sub>30</sub> O <sub>16</sub> MW: 610.1534 	✗	●
772.2071	C <sub>27</sub> H <sub>30</sub> O <sub>16</sub> MW: 610.1534 	✗	●
788.2023	C <sub>27</sub> H <sub>30</sub> O <sub>16</sub> MW: 610.1534 	✗	●
950.2328	C <sub>27</sub> H <sub>30</sub> O <sub>16</sub> MW: 610.1534 	✗	●

317.0657 resulted in the detection of more structurally relevant fragment ions, which matched with the reference flavonoid isohamnetin (Figure 2b). Thanks to this confident substructure match using MS<sup>3</sup> spectral data, we established that part of the structure of the unknown compound had the same structure as the reference, confirming that this unknown compound belongs to the same flavonoid class.

The Mass Frontier 8.0 software was used to process the MS<sup>n</sup> spectral tree data for each juice sample. The software's Joint Components Detection (JCD) algorithm was used to detect unknown compounds from the raw data for each juice, with detected compounds and associated spectral trees then queried against mzCloud's MS<sup>n</sup> spectral library containing mass spectra generated from authentic reference material. Using the "subtree search" functionality, experimental MS<sup>n</sup> trees were compared against MS<sup>n</sup> trees

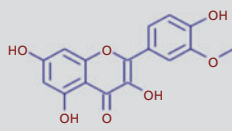
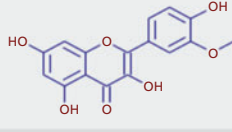
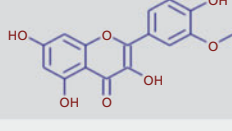
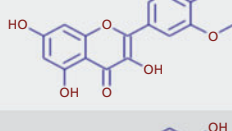
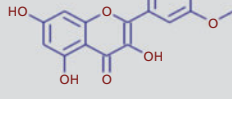
within mzCloud.

For each unknown compound, the greatest overlap between the spectral tree and the library was identified when performing a subtree search. Exact compound matches were made where MS<sup>n</sup> tree matches were found, whereas substructure/subtree matches were made when the compound did not exist in the reference library. These outcomes depended on whether there was an exact or partial MS<sup>n</sup> tree match.

If the MS<sup>2</sup> precursors of the unknown compound and library reference matched, and the spectral tree match between the unknown compound and reference yielded a confidence score of greater than 60, full spectral annotation was achieved. Typically, however, the MS<sup>2</sup> precursor and MS<sup>2</sup> spectra of the unknown compound did not match any library references, due to the limited availability of reference flavonoid standards. The subtree search was able to overcome

this challenge by using the substructure information from the partial MS<sup>n</sup> spectral tree match for true unknown compounds. When a subtree match between an unknown compound and a reference was found, the substructure of the unknown compound was identified to match the reference structure or its substructure. In this way, the software was able to detect true unknown flavonoid compounds using molecular weight, retention time, and substructural data.

The detected compounds that matched both mass lists were selected for further flavonoid structure annotation using the Compound Discoverer 3.0 software. A detected compound with a molecular weight of 742.2320, which matched both mass lists, is shown in Figure 3. Two isomeric flavonoid structures from the Arita Lab 6549 flavonoid structural database, and three isomeric flavonoid structures from the ChemSpider database, were

Molecular Weight	ID Structure/Substructure in MF 8.0	Identified with MS <sup>2</sup> in CD 3.0	Identified with MS <sup>n</sup> and FISH score in CD 3.0
316.0590	C <sub>16</sub> H <sub>12</sub> O <sub>7</sub> MW: 316.0583 	●	●
478.1122	C <sub>16</sub> H <sub>12</sub> O <sub>7</sub> MW: 316.0583 	✗	●
624.1698	C <sub>16</sub> H <sub>12</sub> O <sub>7</sub> MW: 316.0583 	●	●
640.1652	C <sub>16</sub> H <sub>12</sub> O <sub>7</sub> MW: 316.0583 	✗	●
786.2226	C <sub>16</sub> H <sub>12</sub> O <sub>7</sub> MW: 316.0583 	✗	●

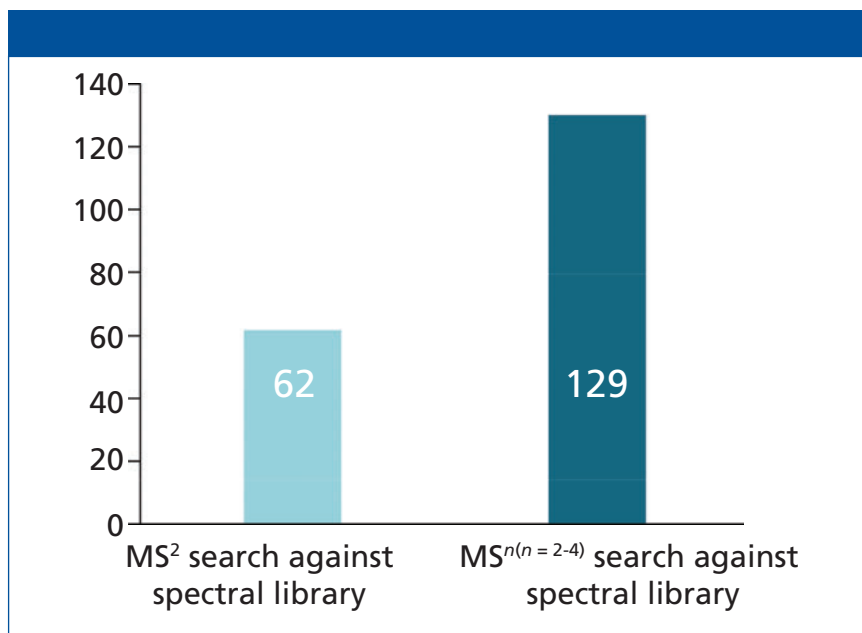


**Figure 4:** Number of annotated flavonoid compounds detected by MS<sup>2</sup>-only and MS<sup>n</sup> workflow.

selected as candidate structures for this compound. These five structure candidates were ranked using the Fragment Ion Search (FISH) scoring algorithm; the software first predicted the fragmentation of the five structural candidates based on known fragmentation rules, before calculating the FISH scores

through matching predicted fragment ions with observed fragment ions from MS<sup>n</sup> data. The structure with the highest FISH score was the best proposed match with the observed fragment ions from the MS<sup>n</sup> data, and was the best structure candidate for the unknown flavonoid class compound. For the fla-

vonoid highlighted in Figure 3, the FISH scoring algorithm annotated the compound as narirutin 4'-glucoside.

## Discussion

Although an MS<sup>n</sup> spectral tree data has previously been used to generate detailed fragmentation pathways for flavonoid annotation (5), MS<sup>n</sup> workflows have traditionally been limited by issues around ease of use. Establishing instrument methods has historically been challenging for nonexpert users, a challenge that has been further compounded by the fact that MS<sup>n</sup> spectral tree data processing has required manual fragment ion assignment. This has proved to be a major process bottleneck, and has required specialist knowledge around flavonoid chemical structure and fragmentation rules.

The structure-specific MS<sup>n</sup> instrument template used in this study enabled the acquisition of high-quality MS<sup>n</sup> data without the need for any specialist expertise. Furthermore, the analysis tools applied in this workflow, including the subtree search function in the Mass Frontier 8.0 software and the FISH scoring algo-

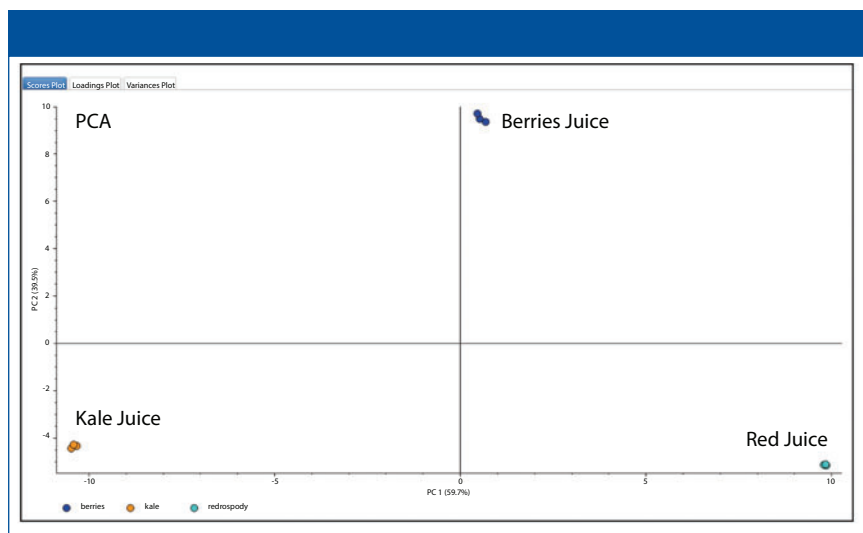


**Figure 5:** Principal components analysis (PCA) of flavonoid compounds identified from the three juice samples.

gorithm in the Compound Discoverer 3.0 software, allow fragment ion information from the  $MS^n$  spectral tree to be processed automatically, without the need for knowledge of specific fragmentation rules.

The new workflow presented here makes full use of the deeper and more structurally relevant fragment ion information generated through  $MS^n$  analysis, enabling more flavonoid compounds to be annotated relative to an  $MS^2$ -only approach. The partial  $MS^n$  spectral tree match results provided valuable substructural information for true unknown compounds; with subtree search, the software identified unknown compounds belonging to the flavonoid compound class that did not have exact references in the mzCloud library, but partial matches of the extensive high resolution fragmentation information within mzCloud.

Tables I and II highlight some of the flavonoids identified by the novel  $MS^n$  workflow, and compare these to the compounds identified using an  $MS^2$ -only approach. Table I demonstrates that, although both methods identified the flavonoid rutin in the juice samples, the  $MS^n$  method was able to identify five additional unknown secondary metabolites of this compound. Similarly, Table II shows that an additional three secondary metabolites of the flavonoid isorhamnetin could be identified using the  $MS^n$  spectral tree data.

In total, the  $MS^n$  spectral tree workflow was able to identify a total of 129 flavonoid compounds in the three fruit and vegetable juice samples analyzed in this study. All 62 flavonoid structures identified by the  $MS^2$ -only approach were found using the  $MS^n$  spectral tree workflow, together with an additional 67 flavonoids that were only detected using the new technique (Figure 4). This represents a twofold increase in the number of annotations relative to the  $MS^2$ -only approach.

The structure-based  $MS^n$  approach presented here also enables simultaneous quantitation of identified flavonoid compounds and statistical analysis. The instrument template was deliberately designed with a short cycle time of 1.2 s to achieve sufficient scan points across the chromatographic peak. This strategy enabled both precise quantitation, while facilitating the acquisition of detailed  $MS^n$  spectral tree data in the same LC-MS run.

By obtaining wider annotation coverage of flavonoid compounds using this approach, a greater number of data points could be obtained for more precise statistical analysis. A hierarchical cluster analysis (HCA) of the detected flavonoids revealed that the kale and berries juice samples contained a greater number of high abundance flavonoids. In contrast, most flavonoids detected from the “red” juice sample were present in low concentrations.

The principal component analysis (PCA) shown in Figure 5 reveals that the three juice samples are well differentiated. The proximity of the points for each replicate analyses highlights the precision of the method. This approach could potentially be used in food analysis workflows to support juice adulteration testing.

## Conclusion

The limited availability of authentic flavonoid reference standards has proven to be a major challenge for flavonoid structure characterization workflows, with existing profiling efforts largely reliant upon manual and time-consuming assignment of  $MS^2$  and higher-order  $MS$  fragmentation data. The novel structure-based  $MS^n$  flavonoid profiling workflow presented overcomes these challenges to deliver comprehensive unknown compound annotation, without the need for in-depth knowledge of flavonoid fragmentation rules. Using this approach to analyze three juice samples, over twice as many flavonoids were annotated compared to an  $MS^2$ -only method. This broad coverage enabled PCA to be performed, highlighting distinct differences in the flavonoid composition of the three juices. This workflow is well-suited for the analysis of juices for food integrity applications.

## References

- (1) A.N. Panche, A.D. Diwan, and S.R. Chandra, *J. Nutr. Sci.* **5**, e47 (2016).
- (2) V.C. George, G. Dellaire, and H.P. Vasantha Rupasinghe, *J. Nutr. Biochem.* **45**, 1 (2017).
- (3) P. Kachlicki, A. Piasecka, M. Stobiecki, and L. Marczak, *Molecules* **21**, 1494 (2016).
- (4) D. Tsimogiannis, M. Samiotaki, G. Panayotou, and V. Oreopoulou, *Molecules* **12**, 593 (2007).
- (5) J.J.J. van der Hoof, J. Vervoort, R. J. Bino, J. Beekwilder, and R.C.H. de Vos, *Anal. Chem.* **83**, 409 (2011).

**Simon Cubbon** is a Senior Global Marketing and Strategy Manager for connected laboratory and software at Thermo Fisher Scientific. Direct correspondence to: [simon.cubbon@thermofisher.com](mailto:simon.cubbon@thermofisher.com)

# Preview of the 67th Conference on Mass Spectrometry and Allied Topics

We present a brief preview of this year's ASMS conference, taking place June 2–6, 2019, in Atlanta, Georgia.

**Cindy Delonas**

**T**he 67th Conference on Mass Spectrometry and Allied Topics is set to take place June 2–6 at the Georgia World Congress Center in Atlanta, Georgia.

## Sunday Events

On Sunday, four tutorial lectures will be given, in two sessions, both starting at 5:00 pm. Tutorial Session I will be chaired by Susan Richardson of the University of South Carolina. Stephen Blanksby of Queensland University of Technology. Gavin Reid of the University of Melbourne will present the first lecture, on lipidomics. At 5:45 pm, Enrico Davoli of the Mario Negri Institute will present the second tutorial, on targeted imaging.

Erin Baker of North Carolina University will chair Tutorial Session II from 5:00 pm to 6:30 pm. “Native Mass Spectrometry” is the topic of the first tutorial, presented by Michal Sharon of the Weizmann Institute. Following that talk, “Data-Independent Acquisition” will be presented by Birgit Schilling of The Buck Institute.

The tutorials are followed by the conference opening plenary lecture at 6:45 pm. Mark Z. Jacobson of Stanford University will present a talk titled “Transitioning the World Energy for All Purposes to Stable Electricity Powered by 100% Wind, Water, and Sunlight.”

A welcome reception will follow the plenary lecture, taking place from 7:45 pm until 9:00 pm in the Poster and Exhibit Hall.

## Monday Award Presentations

Jefferey Shabanowitz will receive the Al Yergey Mass Spectrometry Scientist Award Monday at 4:45 pm. The award recognizes dedication and significant contributions to mass spectrometry-based science by “unsung heroes.” Shabanowitz played a major role in the development of peptide sequence analysis by tandem mass spectrometry.

The John B. Fenn Award for a Distinguished Contribution in Mass Spectrometry will then be presented to John R. Yates III of The Scripps Research Institute. The award recognizes Yates

for his development of automated, large-scale interpretation of peptide tandem mass spectral data. His SEQUEST algorithm laid a critical foundation for the field of proteomics and has enhanced the accuracy and effectiveness of mass spectrometry for understanding important biological and clinical questions. Yates will then give an award lecture.

## Tuesday Award Presentation

The Biemann Medal will be awarded to Sarah Trimpin of Wayne State University at 4:45 p.m. The Biemann Medal is awarded to an individual early in his or her career to recognize significant achievement in basic or applied mass spectrometry. Trimpin's award is for unusual observation of highly charged protein ions in an atmospheric pressure MALDI experiment that led to her discovery that ionization occurs simply bypassing compounds through the inlet of a mass spectrometer.

## Thursday Plenary Lecture

On Thursday, Lilly D'Angelo of Global Food & Beverage Technology Associates will give a plenary lecture at 4:45 p.m. titled “Chemistry of Food and Soft Drinks.”

## Closing Event

A closing event at the Georgia Aquarium gets under way at 6:30 pm on Thursday. Tickets must be purchased in advance by noon Monday. The ticket cost is \$40 per person and includes a dinner buffet, open until 8:00 pm, with dessert and a cash bar available until the close of the event, at 9:30 pm. Tickets also include one drink per ticket for soda, beer, or wine.

## ASMS 2020

The 68th Annual ASMS Conference will be held May 31–June 4 in Houston, Texas. For more information, visit [www.asms.org](http://www.asms.org).

**Cindy Delonas** is the Associate Editor for *Spectroscopy* and *LCCG North America*. Direct correspondence to [CDelonas@MMHGroup.com](mailto:CDelonas@MMHGroup.com)

# PRODUCTS & RESOURCES

## GC-MS thermal desorption system

Gerstel's MPS TD system is designed as a dedicated sampler for automated thermal desorption, thermal extraction, and dynamic headspace analysis. According to the company, the system can process up to 240 samples, and is operated with one integrated method and one sequence table.

**Gerstel, Inc.,**  
Linthicum, MD.  
www.gerstel.com



## Time-of-flight detectors

BiPolar time-of-flight detectors from Photonis are designed to enhance detection efficiency of both positive and negative high-mass ions. According to the company, the detectors have an ion conversion surface that can be biased up to  $\pm 10$  kV, and is available in 18-, 25-, and 40-mm active areas.

**Photonis USA,**  
Sturbridge, MA.  
www.photonis.com



## Hydrogen laboratory server

The Proton OnSite hydrogen laboratory server is designed to use a proton-exchange membrane, electricity, and deionized water to produce up to 18.8 standard liter per min (SLM or SLPM) of ultrahigh-purity hydrogen gas per day. According to the company, the unit senses demand and adjusts production accordingly.

**Proton OnSite,**  
Wallingford, CT.  
www.protononsite.com



## MALDI-TOF mass spectrometer

Shimadzu's MALDI-8020 benchtop mass spectrometer is designed for matrix-assisted laser desorption ionization time-of-flight mass spectrometry (MALDI-TOF MS). According to the company, the system, using linear TOF, enables fast, low-level detection of proteins, peptides, and polymers, among other analytes.

**Shimadzu Scientific Instruments,**  
Columbia, MD.  
www.ssi.shimadzu.com



## HPLC columns

HPLC columns from Hamilton are available with both silica-based and polymeric supports. According to the company, 17 polymeric columns are included for reversed-phase, anion-exchange, cation-exchange, and ion-inclusion separations, as well as 2 silica-based columns for reversed-phase separations.

**Hamilton Company,**  
Reno, NV.  
www.hamiltoncompany.com



## Air valves

Restek's RAVEqc quick connect air valves are designed as a tool-free alternative to bellows or diaphragm valves. According to the company, the air valves reduce the time and variability associated with connecting air canisters to other devices.

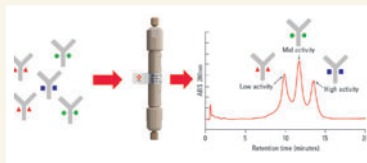
**Restek Corporation,**  
Bellefonte, PA.  
www.restek.com



## Column

Tosoh's TSKgel FcR-IIIa-NPR column is designed for the analysis of IgG glycoforms. According to the company, the stationary phase uses a recombinant human Fc $\alpha$  receptor III as a ligand bound to a nonporous polymethacrylate polymer, providing an elution profile of the glycoprotein that mimics antibody-dependent cellular cytotoxicity activity, which is correlated to the composition of the N-glycans.

**Tosoh Bioscience LLC,**  
King of Prussia, PA.  
www.tosohbioscience.com



## Syringes

VICI Precision Sampling Pressure-Lok analytical syringes are made with polytetrafluoroethylene (PTFE) plunger tips. According to the company, the tips are designed to remain smooth, without the seizing or residue of conventional metal plungers, and have leak-proof seals.

**Valco Instruments Co., Inc.,**  
Houston, TX.  
www.vici.com



# AD INDEX

ADVERTISER	PG#
CDS Analytical .....	31
Gerstel GmbH & Co. KG .....	CV4, 32–33
Hamilton Company .....	3
MilliporeSigma .....	5
Optimize Technologies .....	11
Photonis .....	23
Proton OnSite .....	17
Restek Corporation .....	34–35
Shimadzu Scientific Instruments .....	CV2
Showa Denko America, Inc. ....	CV3
Tosoh Bioscience .....	CVTip, 36–38
VICI Harbor Group .....	7



## CANNABIS science and technology

### Connect with us on Social Media

Join your colleagues in conversation and stay up-to-date on breaking news, research, and trends associated with the legal cannabis industry. “Like” and follow us on Facebook, LinkedIn, Twitter, and Instagram today!



[facebook.com/CannSciTech](https://facebook.com/CannSciTech)



[linkedin.com/groups/12090641](https://linkedin.com/groups/12090641)



[twitter.com/CannabisSciTech](https://twitter.com/CannabisSciTech)



[instagram.com/CannabisScienceTechnology](https://instagram.com/CannabisScienceTechnology)

# EPA Method 8260C Using CDS Analytical 7000C Purge-and-Trap

Xiaohui Zhang, CDS Analytical

*The CDS 7000C purge-and-trap concentrator coupled to a PAL system is a powerful purge-and-trap automation solution. This application demonstrates EPA Method 8260C using the 7000C Purge-and-Trap with the PAL system. A CDS proprietary type X trap shows significant performance improvement against the type K trap.*

CDS Analytical's 7000C purge-and-trap concentrator designed for PAL system fully automates purge-and-trap for the trace measurement of purgeable volatile organic compounds (VOCs) in water, compliant with the official International Standard Organization method DIN-EN ISO 15009, and U.S. EPA method 500 and 8000 series for VOCs in water. In this application note, data are presented that the 7000C PAL system exceeds the performance criteria set of EPA Method 8260C.

Figure 1 is the total ion chromatogram (TIC) of a 200 µg/L calibration standard with internal standard and surrogates containing a total of 65 compounds. Most of the analytes are adequately resolved chromatographically. The chromatogram of the six gases is enlarged in the insert to show the excellent separation and peak shapes.

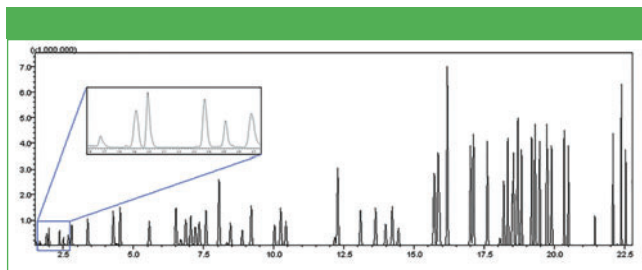


**Figure 1:** TIC of 8260C volatile organic standard mix at 200µg/L with enlarged chromatogram of the six gases.

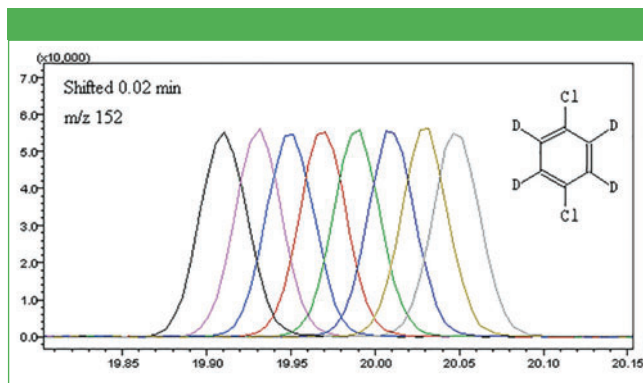


**Figure 2:** Peak overlap of eight 1,4-Dichlorobenzene-d4 runs from the internal standard module. The retention time of each peak has been shifted 1.2 s to show the consistency of the peak shape.

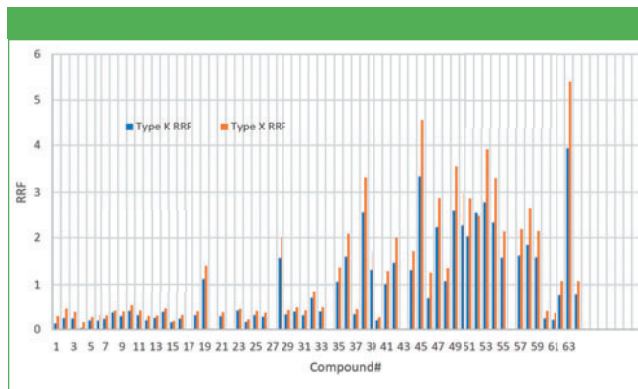


**Figure 3:** RRF comparison for 8260C compounds between type X trap and type K trap.

**Table I: Reproducibility of internal standard addition.**

Compound	Fluorobenzene	Chlorobenzene-d5	1,4-Dichlorobenzene-d4
RSD% (n=8)	1.449	1.478	2.338

The retention time (RT), average relative response factors (Avg RRF), percent relative standard deviation (% RSD) of the initial calibration, method detection limits (MDL), along with method accuracy as percent recovery (% Rec) and as %RSD, are obtained from 0.5 µg/L to 200 µg/L calibration standard, and all analytes exceed the EPA 8260C method requirements. The detailed data for 64 compounds are available in the full-length application note (see website below).

The internal standard module precisely delivered 1 µL of the pre-mixed internal standard solution to each sample. The reproducibility data from eight runs is shown in Table I. An excellent RSD < 2.4% is reported. Figure 2 is the time-shifted overlap of 8 1,4-Dichlorobenzene-d4 runs using the internal standard module.

Although all the data above were collected in a 7000C with a CDS proprietary type X trap installed, a comparison test was performed against the regular type K (Vocarb 3000) trap in the same system. Figure 3 shows the RRF comparison between the two traps for all the 8260C compounds, where an average of 30% increase in RRF from type X trap is observed. Among all the 8260C compounds, 2,2-dichloropropane, which is commonly considered as a testing compound to trace the active site in the flow path, has a 48% increase in RRF from using the type X trap.



**CDS Analytical**

465 Limestone Road, P.O. Box 277, Oxford, PA 19363-0277

tel. (610) 932-3636

Website: [www.cdsanalytical.com/purge-trap-7000c](http://www.cdsanalytical.com/purge-trap-7000c)

# Direct Thermal Extraction Analysis of Food Packaging Material

Laurel Vernarelli, Jackie Whitecavage, and John Stuff, Gerstel, Inc.

Knowledge about packaging and product interaction is of great interest to food manufacturers for the control of product quality over the course of its shelf life. To assess or determine the potential for migration, packaging material can be analyzed using direct thermal extraction (DTE). A small amount of sample, typically 10–50 mg, is placed in an empty thermal desorption tube, and is then heated in the thermal desorption unit under a flow of inert gas, to release volatile and semi-volatile compounds from the sample. The analytes are trapped, and then determined by gas chromatography–mass spectrometry (GC–MS). Direct thermal extraction (DTE) requires very little sample preparation, no solvent is required, and DTE can be used for trace analysis of packaging material. In this work, the technique was used to analyze the packaging of three brands of cream-filled chocolate sandwich cookies and soft and chewy candy bought at a local store. Benzaldehyde was quantified in one brand of soft and chewy candy packaging and found to be  $79 \pm 6$  ng in the 25 mg sample of food packaging. For results on cheese-filled crackers, please consult Gerstel AppNote 203.

## Experimental

### Sample Preparation

A 25-mg portion of packaging was weighed, placed in an empty thermal desorption unit (TDU) tube, and capped with a transport adapter. For the quantification of benzaldehyde, five solutions of the compound in the concentration range of 1–100 mg/L were made in methanol and used to establish an external calibration curve. From

each solution, 1  $\mu$ L was spiked onto a Tenax TA tube and thermally desorbed in the TDU.

### Instrumentation

An Agilent 7890A GC/5977B mass selective detector (MSD), fitted with a multipurpose sampler (MPS), thermal desorption unit (TDU 2) and cooled injection system (CIS) PTV-type GC inlet was used (all from Gerstel®).

### Analysis conditions

For detailed analysis conditions, please see Gerstel application note 203.

## Results and Discussion

### Cream-filled Sandwich Cookie Packaging

DTE was applied to the packaging material for the three samples. Figure 1 shows a stacked view of the resulting chromatograms from the DTE analyses.

In the brand A packaging, the highest levels of extractable compounds were found. Those that could potentially migrate from the packaging to the food included ink-related solvents, such as 1-butoxy-2-propanol and 1-(2-methoxypropoxy)-2-propanol. Evidence of plasticizers used for adhesives were found as sulfonamides and dioctyl adipate. In addition, ethyl vanillin from flavor components, and the preservative butylated hydroxytoluene were also present, having apparently migrated from the product into the packaging material.

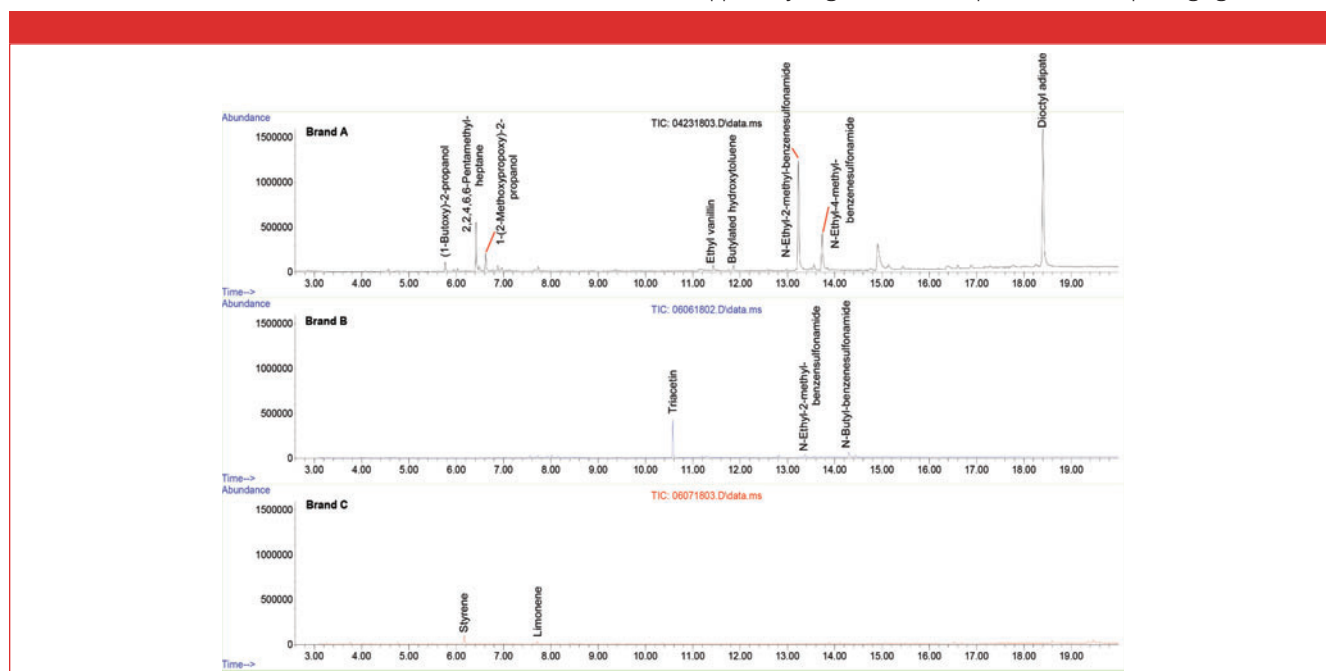


**Figure 1:** Stacked view of total ion chromatograms for direct thermal extraction of packaging material for brand A (top), brand B (middle), and brand C (bottom) cream-filled sandwich cookies.

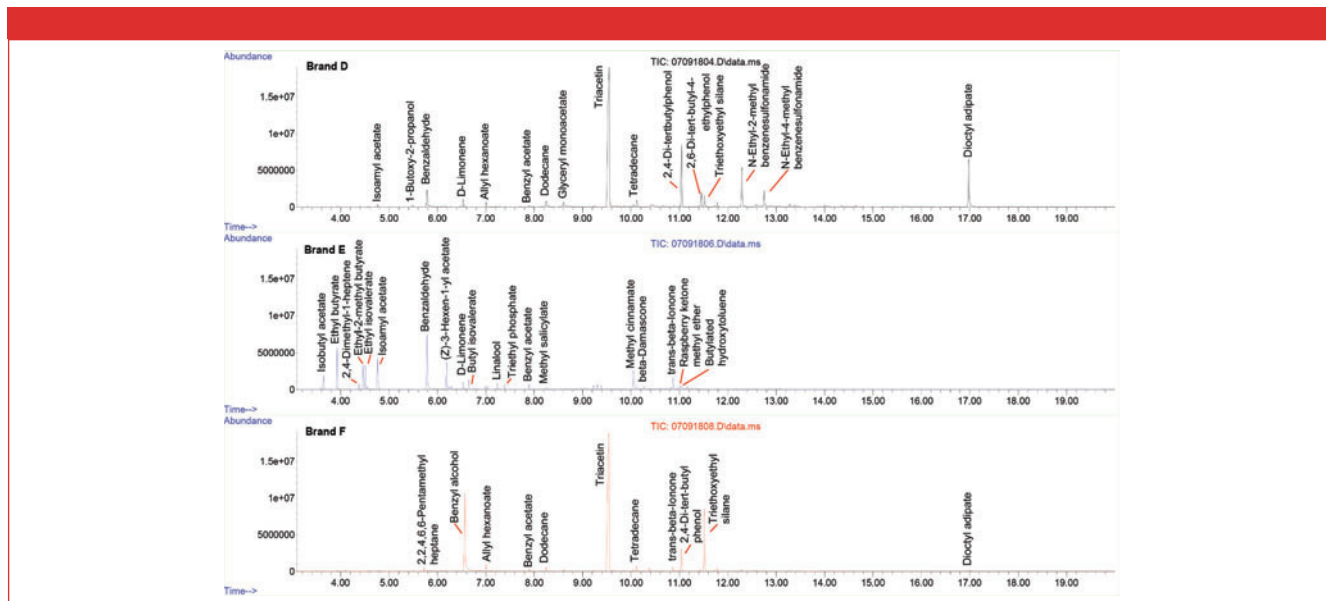


**Figure 2:** Stacked view of total ion chromatograms for direct thermal extraction of packaging material for brand D (top), brand E (middle), and brand F (bottom) soft and chewy candy.

Brand B packaging contains triacetin (a food additive) and vanillin as products that came from the food. Two sulfonamide peaks are also seen in the chromatogram, but at much lower levels relative to brand A. Brand C shows the lowest levels of extractable compounds. The largest two peaks are styrene and limonene.

### Packaging for Soft and Chewy Candy

DTE was applied to the packaging of three brands of soft and chewy candy. Figure 2 shows a stacked view of the resulting chromatograms. All three chromatograms contain flavor compounds from the food product, as well as compounds from the packaging itself. Brands D and F show the highest level of extractable compounds. The chromatograms from brands D and F packaging contain a large amount of the compound triacetin, a carrier solvent for flavor compounds which came from the food product, as well as the flavoring agents allyl hexanoate and benzyl acetate. Both brands D and F packaging contain 2,4-di-tert-butylphenol, an antioxidant, and dioctyl adipate, a plasticizer from the packaging material. In addition, brand D contained two sulfonamide peaks similar to those observed in brand A and B cookie packaging.

The chromatogram for brand E is primarily composed of flavor components resulting from migration from the candy to the packaging: isobutyl acetate, ethyl butyrate, ethyl 2-methyl butyrate, ethyl isovalerate, isoamyl acetate, benzaldehyde, D-limonene, butyl isovalerate, linalool, benzyl acetate, methyl salicylate, methyl cinnamate, beta-damascenone, trans-beta-ionone, and raspberry ketone methyl ether. The chromatogram for brand E also included components derived from the plastic packaging material, 2,4-dimethyl-1-heptene, and an antioxidant, butylated hydroxytoluene.

Quantification: Benzaldehyde was quantified in the brand E packaging using an external calibration curve of the compound spiked onto Tenax TA tubes, which were thermally desorbed in the

TDU. The amount of benzaldehyde in the 25-mg sample of brand E packaging was determined to be  $79 \pm 6$  ng ( $n = 3$ ).

### Conclusions

The results show that DTE is a very good method for quantification as well as assessment of quality defects that may arise due to compounds that migrate from food packaging. The method requires very little sample preparation, and no solvent. The Gerstel MPS/TDU/CIS provides a versatile platform for qualitative analysis of food product packaging. Several techniques can be applied quickly to the same samples providing data for quality control, product development troubleshooting, or competitive analysis. With appropriate use of standards, any of the techniques can be used for quantitative analysis, as illustrated by the quantification of benzaldehyde in the brand E soft and chewy candy packaging.

### Literature

Direct Thermal Extraction Analysis of Food Packaging Material, Gerstel application note No. 203, 2019. <http://www.gerstel.com/pdf/AppNote-203.pdf>

# GERSTEL

**Gerstel, Inc.**

701 Digital Drive, Suite J, Linthicum, MD 21090  
tel. (800) 413-8160, mail: [sales@gerstelus.com](mailto:sales@gerstelus.com)  
Website: [www.gerstel.com](http://www.gerstel.com)

# LC–MS/MS Analysis of Mycotoxins in Peanut Powder in 5.5 Min

Restek Corporation

- Fast analysis for higher sample throughput
- Excellent separation improves accuracy for 12 regulated mycotoxins
- Quick and easy sample preparation (dilute-filter-shoot)

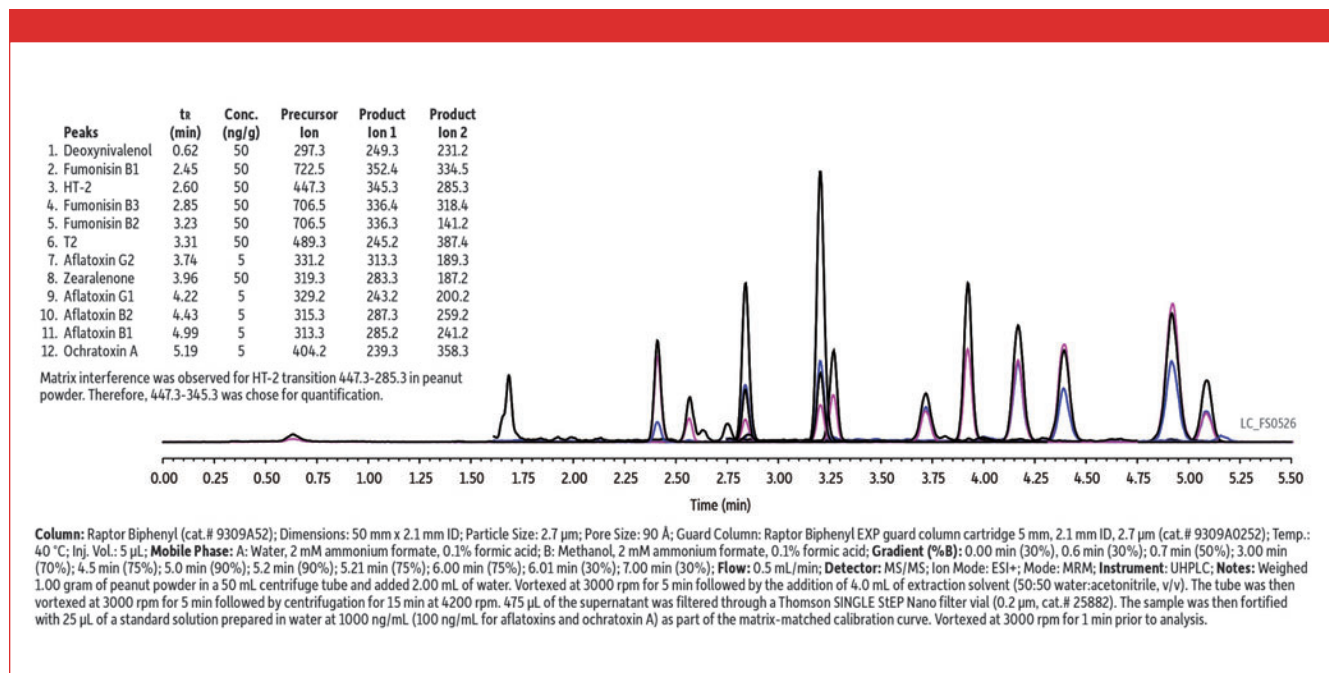
Certain fungi that can grow on agricultural products produce toxic metabolites known as mycotoxins. Modern food processing procedures cannot completely remove these compounds if they are present, so strict monitoring protocols have been established. Although a universal method for the analysis of mycotoxins would allow highly efficient screening, it is very challenging to develop such a method, due to differences in physiochemical properties of mycotoxins, extraction efficiencies, and matrix effects. Zhang and associates published a multi-lab study (1) aimed at providing labs with an analytical procedure that could be broadly applied to the analysis of a variety of mycotoxins in many different matrices. Using that work as inspiration, we developed the following LC–MS/MS method that resolves 12 FDA regulated mycotoxins within the pressure limits of traditional HPLC instruments.

In this example, mycotoxins were analyzed in a peanut powder matrix. The use of a relatively short column format, the selectivity of the Biphenyl stationary phase, and the efficiency of 2.7- $\mu$ m Raptor superficially porous particles provided excellent separations

in a fast 5.5-min analysis (total cycle time of 7 min). A coeluting matrix compound that shared the most abundant MRM transition for mycotoxin HT-2 (447.3-285.3) was observed, so a less abundant transition (447.3-345.3) was selected for quantitation. To increase sensitivity, an ammonium buffer was used to promote better ionization of mycotoxins. The Raptor Biphenyl column worked very well for the 12 mycotoxins studied in the cited work, but for longer compound lists containing isobaric mycotoxins with similar structures, the Raptor FluoroPhenyl phase may be necessary to provide adequate chromatographic resolution. The selectivity of the Raptor FluoroPhenyl column is demonstrated in an analysis of 20 mycotoxins that can be found by visiting [www.restek.com](http://www.restek.com) and entering LC\_FS0511 in the search.

This method showed excellent precision and accuracy for the 12 FDA regulated mycotoxins that were evaluated during a validation study that covered a variety of matrices (including multiple sources of cornmeal and brown rice flour, in addition to the peanut powder example shown here).

Restek would like to thank Dr. Zhang for his technical support during this project.



## Raptor Biphenyl LC Columns (USP L11)

Length	2.1 mm cat.#	3.0 mm cat.#	4.6 mm cat.#
<b>1.8 <math>\mu</math>m Columns</b>			
30 mm	9309232	—	—
50 mm	9309252	930925E	—
100 mm	9309212	930921E	—
150 mm	9309262	—	—
<b>2.7 <math>\mu</math>m Columns</b>			
30 mm	9309A32	9309A3E	9309A35
50 mm	9309A52	9309A5E	9309A55
100 mm	9309A12	9309A1E	9309A15
150 mm	9309A62	9309A6E	9309A65
<b>5 <math>\mu</math>m Columns</b>			
30 mm	—	930953E	—
50 mm	9309552	930955E	9309555
100 mm	9309512	930951E	9309515
150 mm	9309562	930956E	9309565
250 mm	—	—	9309575

## Reference

- (1) K. Zhang, M.R. Schaab, G. Southwood, E.R. Tor, L.S. Aston, W. Song, B. Eitzer, S. Majumdar, T. Lapainis, H. Mai, K. Tran, A. El-Demerdash, V. Vega, Y. Cai, J.W. Wong, A.J. Krynitsky, T.H. Begley, *J Agr Food Chem*, **65**(33) 7138–7152 (2017). <https://www.ncbi.nlm.nih.gov/pubmed/27983809>.



**RESTEK**<sup>®</sup>

**Restek Corporation**  
 110 Benner Circle, Bellefonte, PA 16823  
 tel. (800) 356-1688  
 Website: [www.restek.com](http://www.restek.com)

# Characterization of a TSKgel® FcR-III A-NPR HPLC Column by Top-Down Mass Spectrometry

Tosoh Bioscience

Monoclonal antibodies (mAbs) comprise the largest class of glycosylated protein therapeutics currently on the market, and glycosylation is known to be a major source of mAb heterogeneity. N-glycosylation of IgG-Fc of mAbs is known to impact drug therapeutic mechanism of action (MOA), thus monitoring glycan critical quality attributes (CQAs) is an essential part of biopharmaceutical development. Glycosylation is a critical factor in drug product solubility, kinetics, stability, efficacy, and immunogenicity. Analytical methods utilize a suite of chromatographic modes using high performance liquid chromatography (HPLC) to analyze glycosylation of both intact and digested protein molecules.

The TSKgel FcR-III A-NPR column is a high-performance affinity chromatography column for the analysis of IgG glycoforms. The stationary phase utilizes a recombinant FcR-III A protein bound to a nonporous polymethacrylate polymer. The retention mechanism is based on the interaction between the FcR ligand and the sugar moieties attached to the ASN amino acid in the conserved region of the monoclonal antibody. The resulting elution profile of the glycoprotein mimics ADCC activity, which is correlated to the composition of the N-glycans.

The purpose of this study is to demonstrate the use of mass spectrometry to characterize the elution profile of a typical IgG<sub>1</sub> molecule separation on a TSKgel FcR-III A-NPR column, and verify the observations that certain glycan structures impart higher activity to the monoclonal antibody, especially as it relates to the presence of terminal galactose sugars.

## Experimental HPLC Conditions

### TSKgel FcR-III A-NPR Separation

Column: TSKgel FcR-III A-NPR, 5 µm, 4.6 mm ID × 7.5 cm  
 Instrument: Agilent 1200  
 Mobile phase: A: 50 mmol/L Na citrate, pH 6.5  
 B: 50 mmol/L Na citrate, pH 4.5  
 Gradient: 0 min: 0% B, 20 min: 100% B, 30 min, 100% B  
 Flow rate: 0.85 mL/min  
 Detection: UV @ 280 nm, 25 Hz  
 Temperature: 15 °C  
 Injection vol.: 5 µL  
 Sample: NIST mAb fractions; 5 mg/mL in mobile phase A

## Top-Down MS Characterization

Column: TSKgel Protein C4-300, 3 µm, 2.0 mm ID × 15 cm  
 Instrument: Shimadzu Nexera® XR  
 Mobile phase: A: 0.1% formic acid in water  
 B: 0.1% formic acid in acetonitrile  
 Gradient: 0 min: 10% B, 40 min: 95% B, 50 min: 95% B  
 Flow rate: 0.2 mL/min  
 Detection: Sciex X500B Q-TOF, ESI positive, m/z 900–4000  
 Temperature: 50 °C  
 Injection vol.: 5 µL  
 Samples: NIST mAb fractions; 100 µg/mL in LC–MS water

MS conditions			
Source gas 1	50 psi	Spray voltage	5000eV
Source gas 2	50 psi	Declustering potential	250 eV
Curtain gas	50 psi	DP spread	0 eV
CAD gas	7 psi	Collision energy	10 eV
Source temp	400 °C	CE spread	0 eV
Accumulation time	1 sec	Bins to sum	80

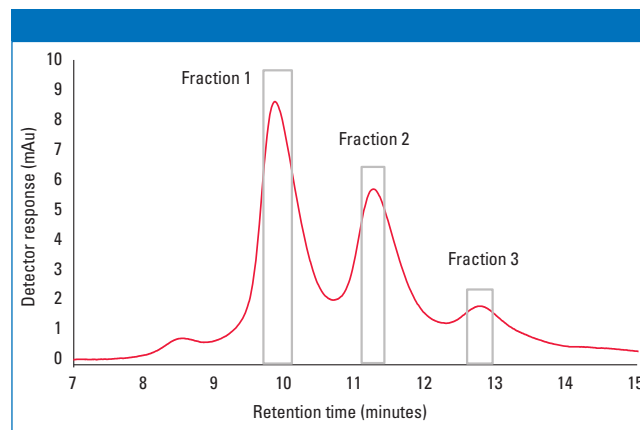


**Figure 1:** Zoomed view of the elution profile of NIST mAb on TSKgel FcR-III A-NPR. The boxes highlighting each peak represent fractions that were collected.

## Results and Discussion

Figure 1 demonstrates the separation of NIST mAb on the TSKgel FcR-III A-NPR column. IgG<sub>1</sub> molecules yield this typical type of elution profile based on glycoform composition that is consistent with ADCC activity. This offers a fast orthogonal chromatographic method for determination of antibody activity and comparisons of antibody heterogeneity.

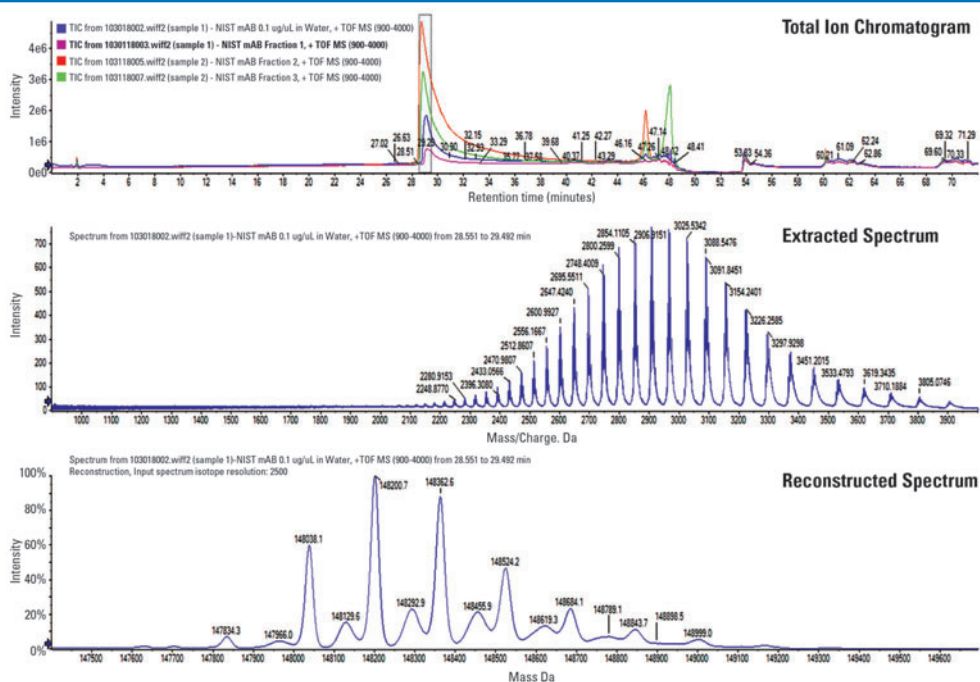


**Figure 2:** The TIC, extracted spectrum, and reconstructed spectrum for a NIST mAb control sample. The glycoforms observed for this sample are in agreement with accepted literature on characterization of this molecule.

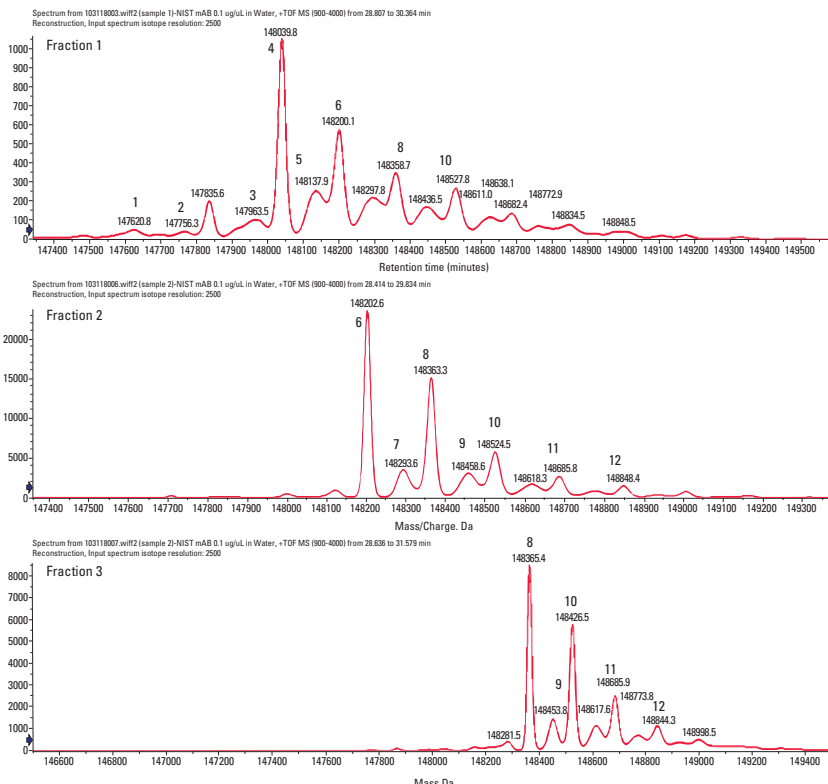


**Figure 3:** Reconstructed spectra for each of the isolated peak fractions, indicating that later eluting fractions have a greater proportion of terminal galactose glycan sugars, consistent with observations of antibody activity and percentage of galactose.

Data for isolated peak fractions in reconstructed spectra (Figure 3)

Peak	Mass	Spray voltage	Peak	Mass	Glycoform
1	147620	GOF/GOF (-2Glc NAc)	7	148292	GOF/G1F (Adduct)
2	147756	GOF/GOF (-Glc NAc)	8	148362	G1F/G1F
3	147966	GOF/G1F (-Glc NAc)	9	148455	G1F/G1F (Adduct)
4	148038	GOF/GOF	10	148524	GOF/G2F (+Hex)
5	148129	GOF/GOF (Adduct)	11	148684	G2F/G2F (+Hex)
6	148200	GOF/G1F	12	148843	G2F/G2F

The three largest eluting peaks were collected and analyzed by offline mass spectrometry. Peak fractions were pooled from successive 25 µg on column injections, concentrated, and buffer exchanged to LC-MS-grade water.

Figures 2 and 3 illustrate analysis of the NIST mAb standard compared against the collected peak fractions. It is observed that each peak has a unique composition of intact mAb glycoforms, and that the selectivity of the stationary phase is based on the amount of terminal galactose units on the glycan moiety. This conclusion agrees with studies that show antibodies with higher amounts of G1- and G2-containing sugars show greater ADCC activity. Because of some peak overlap in the initial separation, there is some overlap of different galactose-containing species in the MS profile, though the general trend between galactose and activity has been confirmed.

### Conclusions

The separation of an IgG<sub>1</sub> molecule was demonstrated using the TSKgel FcR-IIIa-NPR column and peaks from that separation were characterized by high-resolution mass spectrometry. The results support that the stationary phase selectivity is based on the same Fc-glycan/Fc receptor interaction as ADCC activity. The glycoform composition of each peak is consistent with previous published observations on the activity of N-glycan sugars with higher amounts of terminal galactose.

This application demonstrates the efficacy of this approach and characterization data that demonstrate the proof of concept of this chromatographic technique for a fast orthogonal analysis to evaluate mAb ADCC activity, potentially for early cell line development, bioreactor modeling, and lot-to-lot comparability of therapeutic antibodies.

*Tosoh Bioscience and TSKgel are registered trademarks of Tosoh Corporation.*

*Nexera is a registered trademark of Shimadzu Corporation.*



**TOSOH BIOSCIENCE**

TOSOH

**Tosoh Bioscience LLC**

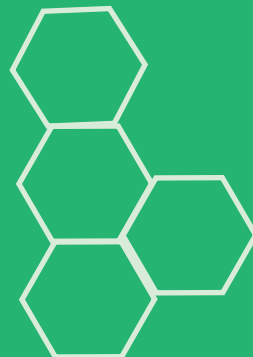
3604 Horizon Drive, Suite 100, King of Prussia, PA 19406

tel. (484) 805-1219, fax (610) 272-3028

Website: [www.tosohbioscience.com](http://www.tosohbioscience.com)

# Shodex™

CAPTURE THE ESSENCE



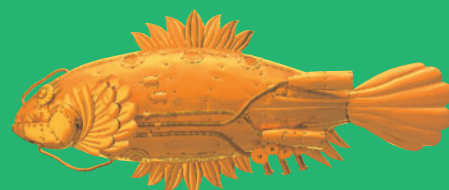
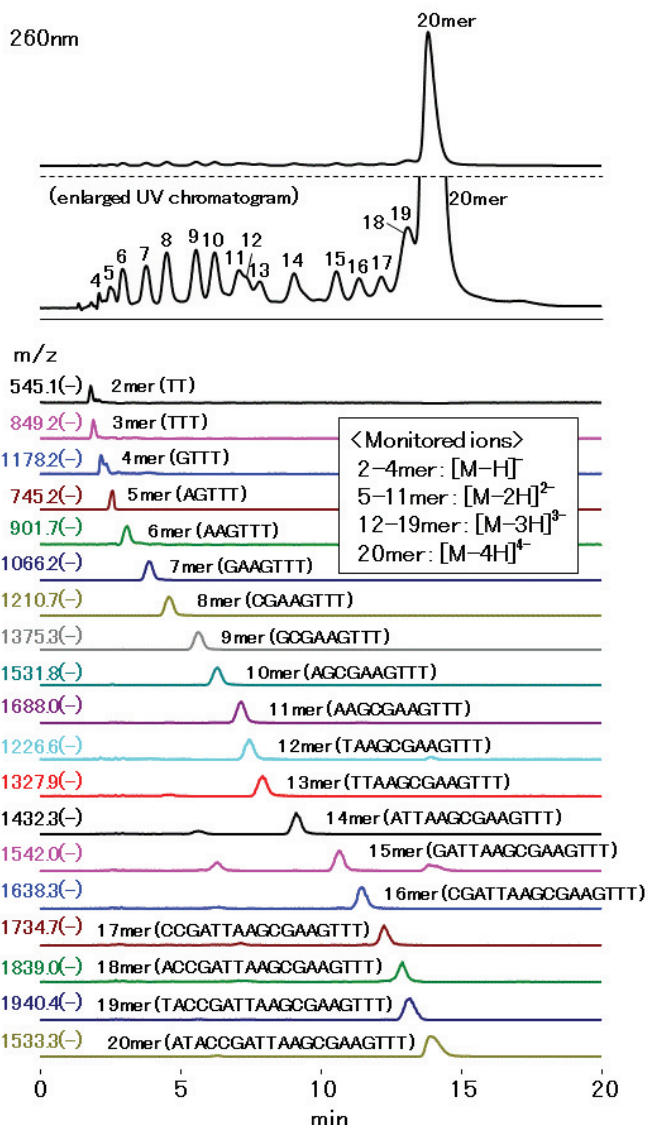
## HILICpak

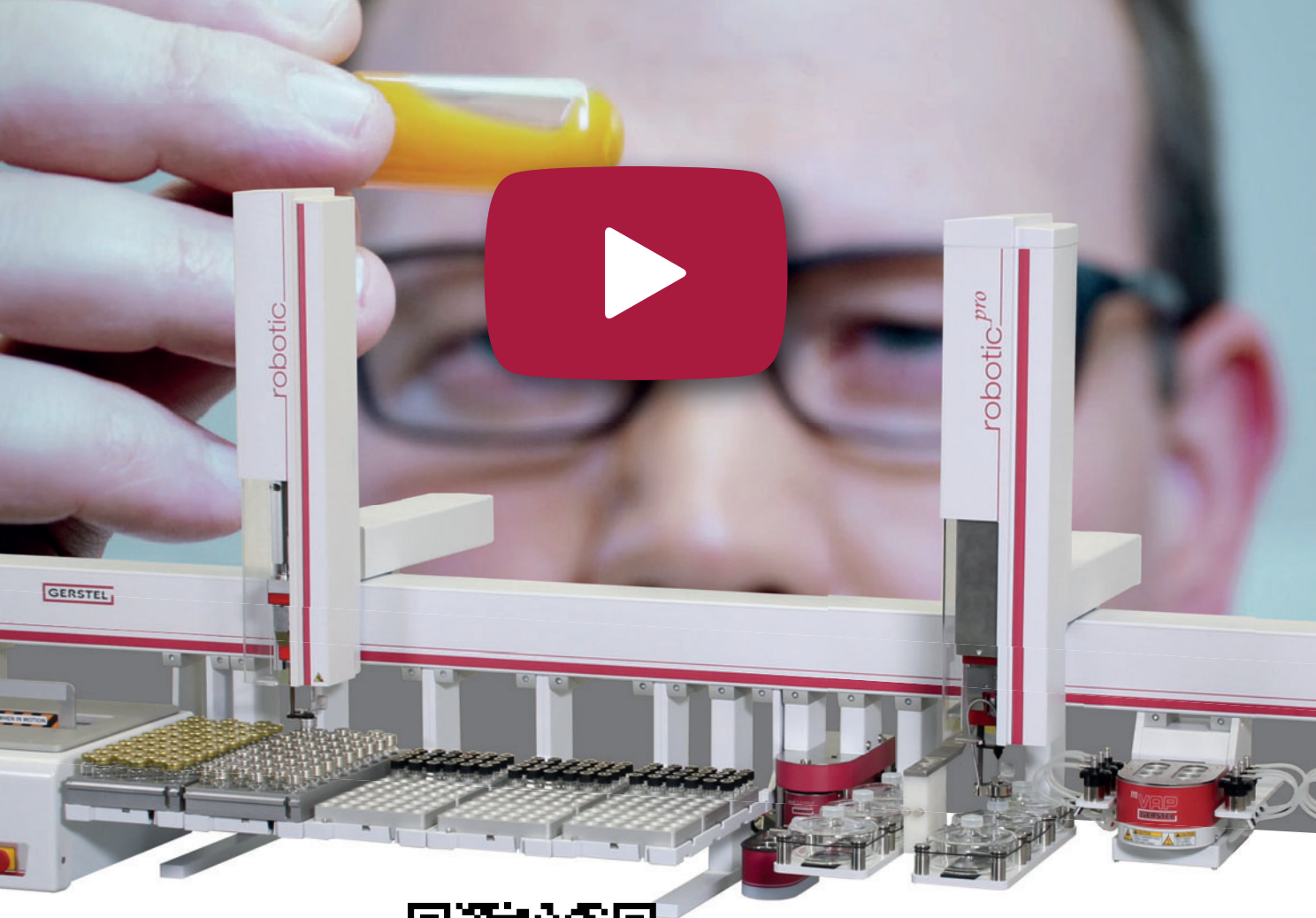
### HILICpak VN-50

- Unpurified oligo DNA analyzed with LC/UV/MS detection
- No ion pair reagent

### Column Specs

- Modified diol groups
- Housed in PEEK





Extraction, derivatization,  
addition of standards



Solid Phase Extraction  
(SPE), Filtration



Batchwise Evaporative  
Concentration (MVP)



Agitation, *quickMIX*



Centrifugation



MAESTRO PrepAhead  
Productivity

## Outstanding Performance

Automated Sample Preparation and Introduction for GC/MS and LC/MS with the GERSTEL MPS in the Lead Role: Efficient, accurate and reliable - automated to your specifications.

Setup and start by mouse-click: Your MPS works day and night, using less solvent and without anyone watching over it.

Intelligently automated GERSTEL Solutions for GC/MS and LC/MS: Dependable Productivity and Less Stress for Laboratory Staff, the Workplace and the Environment.

**What can we do for you?**

**GERSTEL**